The University of Auckland

Galiev, Sh.U., Galiyev, T. Sh.

Eruption of the Universe out of a pre-universe

Auckland

2016

ABSTRACT

Recent results from the Planck satellite, combined with earlier observations from WMAP, ACT, SPT and other experiments do not support the current standard model of cosmology, which combines the Big Bang origin and the inflationary scenario [41-43]. Therefore a few new basic models were constructed so that to avoid the hypotheses of the standard cosmological model. Some researchers began to study the Planck epoch, the earliest period of time of the Universe before the Big Band and the inflation. Some models are based on an idea about a multiverse. The origin of the Universe may be described by the scalar fields since the recent observations favour cosmological models with simple scalar fields.

Here we try to describe mathematically the origin of the Universe as a result of an interaction of scalar fields. Namely, a sequence of solutions of the nonlinear Klein–Gordon equation describes the evolution of pre -universe into the very early Universe, where gravitational forces have not yet emerged.

At first the scalar field, which describes structures of a static part and a dynamic part of pre-universe, is considered. Multidimensional landscapes of the scalar field and the scalar potential of the pre- universe are described. The landscapes consist of ridges and valleys. Multidimensional spherical bubbles oscillate within the valleys (they are potential wells). It is shown that the local interaction of the static and dynamic parts of the landscape can greatly increase energy of certain bubble. As a result, the bubble erupts out of the potential well. We suggest that energy of the bubble can yield our Universe.

Then an influence of quantum fluctuations on the scalar field is studied. They are also described by the nonlinear Klein–Gordon equation. Resonant cases are studied when an influence of the fluctuations increases above some critical level. As a result the bubble escapes out of the pre-universe and forms our Universe. At the same time, the original spacetime is being shredded into fragments having a great energy.

…Thus, we link the origin of the Universe with strongly nonlinear interaction of scalar fields existing in some pre-universe. It is known, that many physical fields can exist simultaneously at the same place. At the same time they do not practically interact with each other. However, due to quantum fluctuations the fields can occasionally interact. The Universe might be originated as a result of similar interaction.

Eruption of the Universe out of a pre-universe

Galiev, Sh.U., Galiyev, T. Sh.

Department of Mechanical Engineering, The University of Auckland,
Private Bag 92019, Auckland 1142, New Zealand: s.galiyev@auckland.ac.nz

Contents

1. Introduction

Existence of the Universe and its origin are some of the greatest puzzles. There were many tales, myths and ideas that attempted to provide an answer. The scientists, however, came up with only a few fundamental theories. We start by briefly introducing some of those concepts.

Up to the middle of the XX century many researchers thought that the Universe always existed and did not change with time. This opinion was supported by the general theory of relativity of Einstein. He found that the Universe is stationary. In particular, it has no beginning and no end. This point of view held in cosmology long time after Einstein [1]. It still has its supporters up to the present time [2, 3]. In particular, models of slowly varying (nearly stationary) Universe without the beginning and the end were suggested.

However, more modern cosmological theories were developed since then.

Debatably, modern theoretical cosmology was based by Alexander Friedman [4, 5]. He started from the fundamental results of Einstein but rejected the static paradigm. As a result he formulated a mathematical theory of the evolutionary Universe, which has the beginning and the end. According to the calculations of Friedman, at the initial moment, which we now call the Big Bang, all matter in the Universe was packed into a single point, where the density is infinite (singularity). Friedman's results were the starting point for many works. In most of them the researchers assumed there being the beginning of the Universe. Lemaître assumed 'the energy of the universe packed in a few or even in a unique quantum' and 'the beginning of the world happened a little before the beginning of space and time' [6]. He formulated the fundamental thoughts. Indeed, the Universe did not necessarily begin from a singularity. May be the Universe passed smoothly through the beginning [2, 3, 7, 8, 9]?

But how did this beginning come about? Perhaps the most original opinion was formulated in [10]. The Universe can be born instantaneously, as a result of a quantum vacuum fluctuation, from 'nothing' along with space and time as a clot of energy and matter. This suggestion opened a way to use physical laws to study the beginning of the Universe's evolution [11-15].

The model [10] was criticized since a vacuum may only exist in some pre-existing spacetime (existing or existed before our Universe). Now it is well known that a vacuum is very different from 'nothing' [16, 17]. The vacuum can have energy. The vacuum cannot be considered an empty place. It is possible to assume that the vacuum of [10] belongs to some pre-existing universe. Over the last few decades several scientific models were developed taking into account a possibility of existence of the pre-universe and some spacetime before the beginning.

The idea of existence of pre-universe or some global multiverse opened up opportunities for constructing theories which are far from models of a single stationary or quasi-stationary universe. One of them is the theory of the eternal inflation. According to it, our universe came into existence along with an infinite number of other universes (multiverse) due to a phase transition in some scalar field [18-20]. The origin resembles the birth of bubbles in boiling water. The emergence of the bubble universe is determined by the quantum fluctuations when the conditions of the scalar field close to the conditions of 'boiling' [21-24]. In this model a bubble universe can collide with another bubble universe [21, 24].

The parallel deep idea in scientific cosmology is that the Universe was born not just once, but multiple times in an endless cycle of fiery deaths and rebirths. These cyclic-universe models were popular in the 1920 -1930 years. But they were replaced by the model of the Big Bang. Now they reappear [25-33]. Perhaps, the most well developed version of this model is presented in [27]. Roughly speaking, it suggests the existence of two universes separated by an extra spatial dimension (parallel universes). The universes exist independently, but periodically collide when the extra dimension disappear. The moment of this collision can be regarded as an analogy of the Big Bang. Thus, the model contains some elements and many results of the Big Bang model and the inflationary scenario. At the same time it additionally takes into account the role of dark matter and dark energy. After the collision the extra dimension increases and these universes diverge. Some researchers speak about single cyclic-universe. Our Universe may have begun as the Big Bounce instead of the Big Bang [34].

Above we described two fundamental approaches to the origin of the Universe. Many new models may be constructed within these approaches. Some of them were developed in recent years [35-40].

For example, the Universe could form as a result of a collapse of a star located in the pre-universe into a black hole [35-37]. The collapsing black hole causes the emergence of a new universe, whose fundamental properties may differ from the pre-universe where the black hole collapsed. Each universe gives a rise to as many new universes as it has black holes. Or our 3-D Universe can emerge from a 2-D reality as some holographic picture [40].

Thus, there are a sufficient number of well-developed theoretical models of the origin of the Universe. However, even the most popular standard cosmological model (the Big Bang model modified by the inflationary scenario) cannot claim that its predictions are fully consistent with the observations [41-43]. In principle, the results of the collisions of the universes or the Big Bounce results can manifest themselves in the cosmic microwave background radiation (CMB) [44-46]. We can assume that the precision of modern experiments and cosmological observations is sufficient to allow us to start testing existing theories. But, for example, up to now traces of the collisions are not detected [47]. The latest experiments did not support the holographic universe idea too [48].

At the same time we think that the important results of the standard cosmological model are, perhaps, best at explaining many observations. This standard model is based on Einstein's equations rewritten for homogeneous and isotropic spacetime. However, the latest observations [43, 47] did not support the above assumptions. As a result, the standard model became a slippery concept not only because of the singularity at the beginning. It is possible to improve this model using modified Einstein's equations [3]. But in this case, the model becomes very complex. Some researchers think that what we need now a simple, radical idea that will point towards new approaches to the puzzles of the origin of the Universe.

It is known that quantum effects play important roles at the very early Universe [6, 8, 10, 15, 22]. Sometimes, these effects may be described by scalar field equations. Can these equations describe the origin of the Universe [8]? On the whole, an idea of using scalar equations is well known in cosmology [18, 49-52]. Practically, all cosmologists use scalar fields in their theories [53-57]. In particular, an ordinary differential equation describing a scalar field was used in [2] so that to model the origin of the Universe. This formation from pre- universe was studied with the help of the nonlinear Klein–Gordon equation (NKGE) in [58-60].

In this research the sequence of solutions of NKGE describes the evolution of pre -universe into the very early Universe, where gravitational forces have not yet emerged.

At first (section 1) the scalar field, which describes structures of a static part and a dynamic part of pre-universe, is considered. Multidimensional landscapes of the scalar field and the scalar potential of the pre-universe are described. The landscapes consist of ridges and valleys. Multidimensional spherical bubbles oscillate within the valleys. It is shown that the local interaction of the static and dynamic parts of the landscape can greatly increase energy of certain bubble. As a result, the bubble erupts out of the valley (the potential well). We suggest that energy of the bubble can yield our Universe.

Then an influence of quantum fluctuations on the scalar field is studied. They are also described by the nonlinear Klein–Gordon equation. Cases are studied when the fluctuations increase above some critical level. As a result the bubble can erupt from the potential well. Namely, the bubble escapes out of the pre-universe and forms our Universe. At the same time, the original spacetime is being shredded into fragments having a great energy. According to [58-60] the strongly nonlinear oscillations of the fragments radiate particles with enormous energy, which form a new 4-dimensional spacetime and our Universe.

Certain results presented in [58-60] are additionally developed in this research.

2. Scalar field dynamics of a pre-universe

The fields themselves are not 'made of' anything – fields are what the world is made. At the same time, apparently, fields are often the easiest way to describe different natural phenomena. In particular, field theories are often used for purposes of introduction of novel concepts and techniques.

2.1. Basic equation and relations

The pre-universe model is described here using nonlinear Klein-Gordon equation (NKGE). It is known that this equation describes a wide variety of physical phenomena such as wave propagation in different artificial and natural systems and the 'birth' of spinless particles in relativistic quantum mechanics. Above we stressed that this equation play the fundamental pole in certain cosmological models.

Versions of NKGE. We assume that there is nothing in the pre-Universe except the scalar field. Let it be described by NKGE in the following form

$$\hat{\Phi}_{tt} - c_*^2 \sum_{i=1}^{I} \hat{\Phi}_{ii} = -\partial V(\hat{\Phi}) / \partial \hat{\Phi} . \qquad (1)$$

Here c_* denotes a constant, I is an integer value ($I \geq 1$) and V is the scalar field potential. The indexes denote the differentiation; $\hat{\Phi}_{tt} = \partial^2 \hat{\Phi} / \partial t^2$, $\hat{\Phi}_{ii} = \partial^2 \hat{\Phi} / \partial x_i^2$, here x_i are the rectangular cartesian coordinates. the nonlinear equation (1) describes the wide spectre of the massless and spinless scalar fields inside the multidimensional spacetime.

We stress that the rectangular cartesian coordinates are used. These coordinates were used widely for description of complex processes in different arias of physics. In particular, turbulent processes are described often using these coordinates. Recently the collision of universe was modelled with the help of the cartesian coordinates [46, 57, 61]. We note that the Friedmann-Robertson-Walker metric is used traditionally for the study of the homogeneous and isotropic Universe at the earliest epoch of its evolution. But this metric is not applied to massless scalar fields.

Different expressions for the function *V* can be found in many books and papers. We assumed that

$$V(\hat{\Phi}) = \tfrac{1}{2} m^2 \hat{\Phi}^2 - \tfrac{1}{4} \lambda \hat{\Phi}^4 . \qquad (2)$$

Here m^2 and λ are constants. A solution of (1) is represented as a sum,

$$\hat{\Phi} = \overline{\Phi} + \Phi + \lambda_f f . \qquad (3)$$

Here $\overline{\Phi}$ is a stationary part and Φ is a dynamic part of the scalar field, f takes into account the quantum fluctuations, λ_f is a constant. Using (3) we obtain from (1) equations for $\overline{\Phi}$, Φ and f :

$$-c_*^2\sum_{i=1}^{I}\ \bar{\Phi}_{ii} = -m^2\bar{\Phi} + \lambda\bar{\Phi}^3, \tag{4}$$

$$\Phi_{tt} - c_*^2\sum_{i=1}^{I}\ \Phi_{ii} = -m^2\Phi + \lambda[3\bar{\Phi}^2\Phi + 3\bar{\Phi}\Phi^2 + \Phi^3 + 3\lambda_f^2(\bar{\Phi}+\Phi)f^2], \tag{5}$$

$$f_{tt} - c_*^2\sum_{i=1}^{I}\ f_{ii} = -m^2 f + \lambda\lambda_f^2 f^3 + 3\lambda(\bar{\Phi}+\Phi)^2 f\ . \tag{5.1}$$

The equations (5) and (5.1) are focused on the interaction of the fields.

New variables and a simplified model of NKGE. We can not tell what the pre-universe looked like. However, we can assume that some structures inside the pre-universe are similar to the widely accepted form of the very early Universe. We assume that the pre-universe contains multidimensional spherical structures. The following new independent variables are used to describe these structures and different scenarios of the evolution of the scalar field:

$$\eta = -\bar{K}\sum_{i}^{I}\sin^2\vartheta x_i\ ,\ \xi = R^* + B\sin^2\omega t - K\sum_{i}^{I}\sin^2\vartheta x_i\ . \tag{6}$$

Here $\bar{K} = \bar{K}(x_i,t)$, $\vartheta = \vartheta(x_i,t)$, $R^* = R^*(x_i,t) > 0$, $B = B(x_i,t)$, $\omega = \omega(x_i,t)$ and $K = K(x_i,t)$. Let us assume that the dependence of these coefficients from coordinates and time is very weak. It is accepted that the coefficients $\bar{K}$, ϑ, R^*, B, ω are constants considering any local structures of the scalar field. We stress that the values η and ξ are independent. At the same time these values may be equal

$$\eta = \xi\,, \tag{7}$$

if

$$t = \omega^{-1}\arg\sin\sqrt{[(K-\bar{K})\sum_{i}^{I}\sin^2\vartheta x_i - R^*]B^{-1}}\ . \tag{8}$$

In particular, if $x_i = 0$, we have

$$t = \omega^{-1}\arg\sin\sqrt{-R^*/B}\ . \tag{9}$$

Thus, cases may be when the fields $\bar{\Phi}$ and Φ interact. Similar cases are very important for this research. Using (6) we can find expressions $\bar{\Phi}_{tt}$, $\bar{\Phi}_{ii}$, Φ_{tt} and Φ_{ii}. For example,

$$\Phi_{tt} = \tfrac{1}{2}\omega^2B^2\Phi_{\xi\xi}(1-\cos 4\omega t) + 2\omega^2B\Phi_{\xi}\cos 2\omega t\,, \tag{10}$$

$$\Phi_{ii} = \vartheta^2K^2\Phi_{\xi\xi}\sin^2 2\vartheta x_i - 2\vartheta^2K\Phi_{\xi}\cos 2\vartheta x_i\,. \tag{11}$$

Then, we will ignore in (10), (11) the terms explicitly dependent on the harmonics. In this case, we rewrite equations (4) and (5) using (6):

$$\tfrac{1}{2}c_*^2\vartheta^2\bar{K}^2 I\bar{\Phi}_{\eta\eta} - m^2\bar{\Phi} + \lambda\bar{\Phi}^3 = 0, \tag{12}$$

$$\begin{aligned}&\tfrac{1}{2}(\omega^2 B^2 - c_*^2\vartheta^2 K^2 I)\Phi_{\xi\xi} + m^2\Phi - \lambda\Phi^3 - 3\lambda\lambda_f^2\Phi f^2 = \\ &\lambda[3\bar{\Phi}^2\Phi + 3\bar{\Phi}\Phi^2 + 3\lambda_f^2\bar{\Phi}f^2]\delta(\eta-\xi).\end{aligned} \tag{13}$$

Here $\delta(\eta-\xi)$ is the Dirac delta function (the impulse function). We mean that $3\bar{\Phi}^2\Phi + 3\bar{\Phi}\Phi^2 + 3\lambda_f^2\bar{\Phi}f^2 \neq 0$ if $\xi = \eta$. Thus, the left hand side term of (12) may be considered as an instantly acting source which is determined by the interaction of the fields $\bar{\Phi}$ and Φ. If $\xi \neq \eta$ then

$$\tfrac{1}{2}(\omega^2 B^2 - c_*^2\vartheta^2 K^2 I)\Phi_{\xi\xi} + m^2\Phi - \lambda\Phi^3 = 3\lambda\lambda_f^2\Phi f^2. \tag{14}$$

.

If the quantum fluctuations are ignorable then (14) yields

$$\tfrac{1}{2}(\omega^2 B^2 - c_*^2\vartheta^2 K^2 I)\Phi_{\xi\xi} + m^2\Phi - \lambda\Phi^3 = 0. \tag{14.1}$$

.

We simplify the problem to the solution of the ordinary differential equations. In general, this approach is widely used in cosmology for the modelling of dynamics of scalar fields [10, 12, 16-19]. This approximation allows to describe observations and to identify main trends in the development of fundamental processes.

We think [58-60] that some solutions of NKGE can describe the strict sequence of stages of an eruption of the Universe out of some pre-universe. In particular, the solutions should explain an appearance of the initial energy of the Universe. Possible it is a result of the interaction of the fields. But how can they interact ?

We will consider the equation (13) as a simple example of this interaction. In particular, this equation describe very localized interaction of the static and dynamic parts of the scalar field.

We emphasize that very strongly nonlinear fields will be considered, when the coefficient λ varies within very wide limits. In particular, cases will be considered when λ changes from 10^{-120} (see Fig. 14) to 10^{20}. At the same time we stress that according to [50, 52, 41] λ typically has the order from 10^{-13} to 10^{-15} in modern cosmology.

Remarks. The expression ξ (6) can be compared with the Minkowski formula linking time and space. Indeed, if $R^* = 0$ and ωt, ϑx_i are very small, the expression ξ describes the distance from arbitrary point of spacetime to the point $t = 0$, $x_i = 0$.

We used the variables t, x_i and η, ξ (6). We will assume, for the most part, that the scalar field and its corresponding derivatives are finite and continuous function of these variables. At the same time we will consider also cases of exceptions, when the equation (13) has discontinuous solutions.

2.2. Basic solutions

We stress that in spite of the observational triumphs, this standard model remains an unfinished work of art. Many of its late-time successes can be traced to the initial conditions postulated for very early stages of the Universe. The model assumes that the Universe had to start with certain properties that have never been successfully explained by the fundamental physics. So that to explain new observational data, researchers are introducing new and new suggestions which are not fully supported by observations, experiments and the results of fundamental physics. As a result the initially simple Big Bang theory became quite complex.

In contrast with this we hope [58-60] that some solutions of NKGE can describe the strict sequence of stages of an eruption of the Universe out of some pre-universe. In particular, the solutions should explain an appearance of the initial energy of the Universe. Possible it is a result of the interaction of scalar fields. But how can they interact ?

Here we will consider the equation (13) as a simple example of this interaction. Here we will study very localized interaction of the static and dynamic parts of the scalar field.

The static part. First we look for an expression for the static part of the scalar field. The localized exact solution of (12) are sought in the form of the solitary waves (solitons):

$$\bar{\Phi} = \bar{A}\,\mathrm{sech}\,\eta\,. \tag{15}$$

The equation (12) yields

$$[\tfrac{1}{2}c_*^2\vartheta^2\bar{K}^2 I(\sec h\xi - 2\sec h^3\xi) - m^2\,\mathrm{sech}\,\xi + \bar{A}^2\lambda\,\mathrm{sech}^3\,\xi]\bar{A} = 0. \tag{16}$$

Using (16) we found three values for $\bar{A}$:

$$\bar{A}_0 = 0\,,\quad \bar{A}_+ = \sqrt{2}\lambda^{-0.5}m\,,\quad \bar{A}_- = -\sqrt{2}\lambda^{-0.5}m \tag{17}$$

and

$$\vartheta^2\bar{K}^2 = 2m^2c_*^{-2}I^{-1}. \tag{18}$$

Thus, the three solutions (15), (17) for the static part of the field are found.

The dynamic part. Now we consider the dynamic part. Let

$$\Phi = A\,\mathrm{sech}\,\xi\,. \tag{19}$$

Substituting these expression into (13) we have after simple calculations

$$[\tfrac{1}{2}(\omega^2 B^2 - c_*^2 \vartheta^2 K^2 I)(\sec h\xi - 2\sec h^3\xi) + m^2 \operatorname{sech}\xi - A^2\lambda \operatorname{sech}^3\xi$$
$$-\lambda(3\overline{A}^2 \operatorname{sech}^2\eta \operatorname{sech}\xi + 3\overline{A}\operatorname{sech}\eta A \operatorname{sech}^2\xi)\delta(\eta-\xi)]A = 0. \tag{20}$$

The equation (20) yields

$$\tfrac{1}{2}(\omega^2 B^2 - c_*^2 \vartheta^2 K^2 I) = -m^2 . \tag{21}$$

In this case the equation (20) determines

$$A_0 = 0 \tag{22}$$

and

$$A_{\pm} = \tfrac{1}{2}[-3\overline{A}\delta(\eta-\xi) \pm \sqrt{-3\overline{A}^2\delta(\eta-\xi) + 8\lambda^{-1}m^2}\,]. \tag{23}$$

1. *No interaction.* If $\xi \neq \eta$ we have

$$A_+ = \sqrt{2}\lambda^{-0.5}m, \quad A_- = -\sqrt{2}\lambda^{-0.5}m. \tag{24}$$

Thus, if $\xi \neq \eta$, the expressions for $\overline{\Phi}$ (see (15) and (17)) and Φ (see (19), (22) and (24)) are formally the same. Using these solutions we can construct 9 expressions for the scalar field (3). For example, if we assume $\overline{A} = \overline{A}_-$ (17) and $A = A_-$ (24), then

$$\hat{\Phi} = -\sqrt{2}\lambda^{-0.5}m(\operatorname{sech}\eta + A\operatorname{sech}\eta). \tag{25}$$

2. *Interaction* ($\xi = \eta$). But the situation changes in the points of the interaction of the static and dynamic parts of the field. In particular, if $\overline{A} = \overline{A}_+ = \sqrt{2}\lambda^{-0.5}m$ (17), then (23) yields two expressions for *A*:

$$A_{1-} = -2\sqrt{2}\lambda^{-0.5}m \quad \text{and} \quad A_{1+} = -\sqrt{2}\lambda^{-0.5}m. \tag{26}$$

If $\overline{A} = \overline{A}_- = -\sqrt{2}\lambda^{-0.5}m$ (17), then

$$A_{2+} = 2\sqrt{2}\lambda^{-0.5}m \quad \text{and} \quad A_{2-} = \sqrt{2}\lambda^{-0.5}m. \tag{27}$$

Thus, the expression of the dynamic part of the scalar field changes strongly if there is the interaction. For example, instead (25) we have for the case (27) that

$$\hat{\Phi} = (\overline{A}_- + A_{2-})\operatorname{sech}\eta = 0, \tag{28}$$

or

$$\hat{\Phi} = (\overline{A}_- + A_{2+})\operatorname{sech}\xi) = \sqrt{2}\lambda^{-0.5}m\operatorname{sech}\xi. \tag{29}$$

At the point $\xi = \eta$ there is the jump from negative to positive values of the field. We will link the origin of the Universe with similar jumps. The amplitudes of the parts are determined by the values m^2 and λ. Values ϑ, $\overline{K}$, B, ω and K are not completely determined by (18) and (21). We will consider these values as arbitrary. From (18) and (21) follows that

$$K^2 = \omega^2 B^2 c_*^{-2} \vartheta^{-2} I^{-1} + \overline{K}^2 \tag{30}$$

We have $K^2 > \overline{K}^2$ in (6).

We can not really know what are those scalar fields represented by the solutions. We can only see that the solutions determine different types of the dynamic parts of the scalar field. The evolution of this part is most important subject of our research. Apparently these parts may be interpreted as different vacuums [20, 50, 63], however we will not study possibility this interpretation. We will call of them as positive ($A = A_+$ (24)), negative ($A = A_-$ (24)) and zero ($A = A_0$ (22)) dynamic fields.

2.3. Two-dimensional maps of landscapes of the pre-universe

How can we interpret the solutions and expressions written using the variables η and ξ? Let us return to the cartesian coordinates.

At first we consider the landscape of the scalar field so that to appreciate its dynamics. Generally speaking, using the solutions (15) and (19) we can construct smooth as well as discontinuous landscapes. Here a smooth landscapes are considered. Assuming $A = \overline{A} = A_- = -\sqrt{2}\lambda^{-0.5} m$ ((17), (24)) and using (3) we have (25),

$$\hat{\Phi} = -\sqrt{2}\lambda^{-0.5} m(\operatorname{sech}\eta + \operatorname{sech}\xi). \tag{31}$$

The expressions (31) and (2) allow us to calculate the scalar function and the scalar potential. In particular, the expression $\hat{\Phi}$ (31) determines a landscape of the scalar field which is described by static and dynamic parts. We stress that if η and ξ are very large then $\hat{\Phi} \approx 0$.

For simplicity, the two-dimensional landscapes will be calculated. In Figs. 1 and 2 the results of the model calculations are presented. It is assumed that $R^* = 5$, B =25, $\omega = 1$, $K = 300$, $\vartheta = 0.15$ and $\overline{K} = 0.85$. We stress that $K = 300$ is used. In this case, the dynamical part describes a structure having a very thin wall.

The landscape of the scalar field calculated according to (31) is shown in Fig 1 (left). For simplicity we assume that $\sqrt{2}\lambda^{-0.5} m = 1$. The stationary part of the scalar field describes the landscape which consists of ridges (hills) and valleys (Fig. 1 left). The highest value of the function is reached at the top of the hills.

The dynamical part of the field disturbs the stationary picture in the valleys where a thin ring radially oscillates (Fig. 1 right). This ring may be named as the oscillon [63,64].

This oscillon corresponds to a multidimensional oscillating bubble (sphere, clot) which can have a very thin wall. The lowest value of the dynamic field (negative field) is reached in this wall. Within the bubble $\Phi \approx 0$, if the wall is very thin ($K \to \infty$).This case is certain analogue of the well-known thin-wall approximation [63, 64].

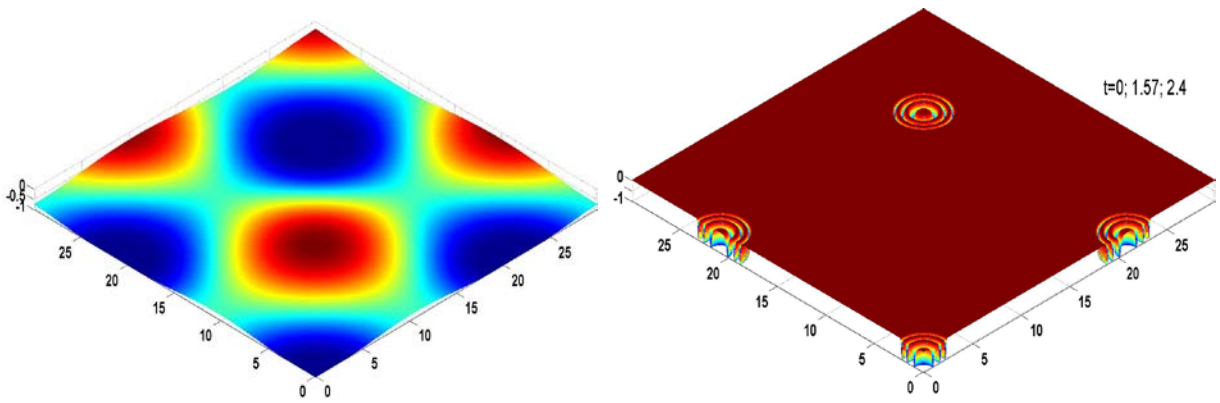

Fig. 1. The static (left) and dynamic (right) two-dimension maps of the landscape of the scalar field. The dynamic landscapes were calculated at three dimensionless moments of time: 0, 1.57 and 2.4.

Substituting (31) into (2) we approximately find that

$$V(\hat{\Phi}) = \lambda^{-1} m^4 [(\operatorname{sech}\eta + \operatorname{sech}\xi)^2 - (\operatorname{sech}\eta + \operatorname{sech}\xi)^4]. \qquad (32)$$

The expression (32) determines a landscape of the scalar potential (Fig. 2 right) which takes into account static and dynamic parts of the field. For the calculation we assume that $\lambda^{-1} m^4 = 1$ in (32).

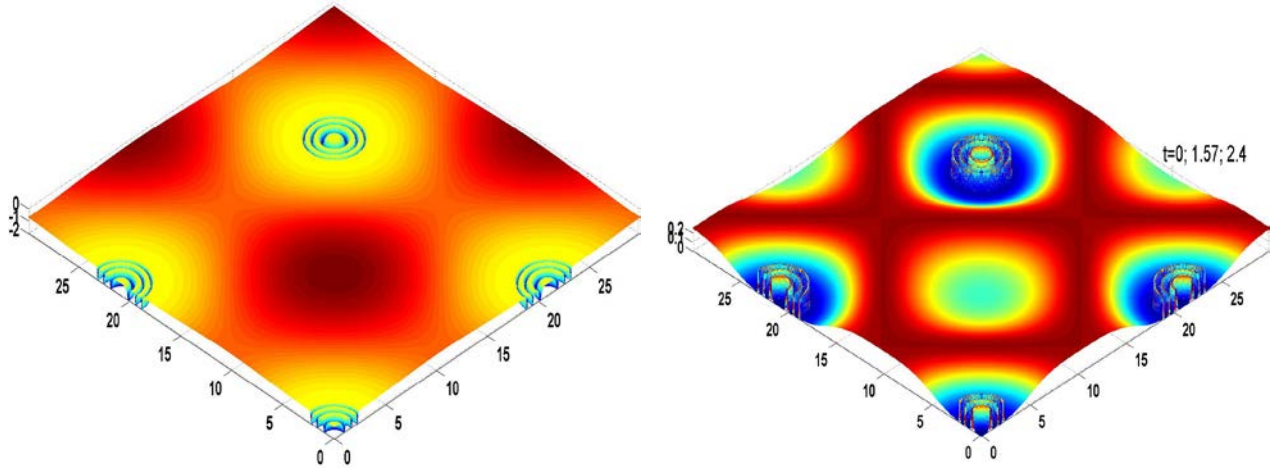

Fig. 2. The two-dimensional maps of the combined landscapes. The map of the scalar field (left) and the map of the scalar potential (right). The calculations were made at three dimensionless moments of time: 0, 1.57 and 2.4.

The dynamic part (bubble, sphere, clot) of the scalar field oscillates inside of the scalar potential well (Fig.2 right). This part cannot escape from the well unless it is given a large enough energy influx. We assume that similar landscapes describe the scalar potential of some pre-universe.

We think that the calculations describe qualitatively a structure of some pre-universe. According to our model the pre-universe is a system of infinite number of bubbles oscillating in potential wells. The hills and wells are described by the static part of the scalar field. The bubbles correspond more to the dynamic part. The bubbles may be slightly different from each other since the coefficients in (6) may be different slightly. The bubbles contain a scalar field which may be very close to the zero field. The negative field is concentrated in the surface of the bubbles. We can compare the inner field with pressure of gas in some elastic bubble and the negative field may be some analogue of the surface tension. The negative field (which was described as $-\sqrt{2}\lambda^{-0.5} m \operatorname{sech}\xi$ ((19), (24)) does not allow to increase strongly the volume of the bubble. We can use another parallel for the oscillating bubbles. Let us suggest that the 'potential' energy of bubbles transforms partly into 'kinetic' energy and vice versa. In other words, the zero field (pressure) transforms partly into the negative field (tension) and back.

Generally speaking, the bubbles might be very small (the value R^* may be like the Planck's scale dimension) and the amplitude of the oscillations might be also extreme small.

3. Description of quantum perturbations

How can we introduce a quantum action so that to describe the evolution of an element of the pre-universe into the Universe?

According to the Heisenberg's uncertainty principle, the wave packets of energy instantly and spontaneously are forming and quickly are disappearing within vacuum. This process is known as 'quantum fluctuations'. We assume that these localized fluctuations occur in the pre-universe. The problem is to describe an influence of the perturbations on the scalar field.

3.1. Quantum perturbations and free nonlinear oscillations in the potential well

Up to this moment we did not stress the influence of quantum fluctuations on the origin of the Universe. We studied above the geometrical structures of the dynamical landscape of some pre-universe. The important particularities of the structures are the potential wells containing oscillating bubbles of the scalar energy.

Now we suggest additionally that there are actions of quantum fluctuations on the structures. These fluctuations are described by the equation (5.1). The fields $\overline{\Phi}$ and f are considered as separable. Then the equation (5.1) is rewritten using the variable ξ (6). As a result we have the equation similar to (14):

$$\tfrac{1}{2}(\omega^2 B^2 - c_*^2 \vartheta^2 K^2 I) f_{\xi\xi} + m^2 f - \lambda\lambda_f^2 f^3 = 3\lambda\Phi^2 f \,. \tag{33}$$

The solution is written in the form:

$$f(\xi) = \tilde{A}\,\mathrm{sech}\,\Omega\xi \sin(n\bar{\Omega}\xi + \phi)\,. \tag{34}$$

Here Ω, $\bar{\Omega}$ and φ are constants, n is the integer number (n=0, 1, 2, 3,…). According to (19)

$$\Phi = A\,\mathrm{sech}\,\Omega\xi\,. \tag{34.1}$$

The expressions (34), (34.1) are substituted into the equation (33). Then we find that

$$\begin{aligned}
&\tfrac{1}{2}\tilde{A}(\omega^2 B^2 - c_*^2 \vartheta^2 K^2 I)[2\Omega^2\,\mathrm{sech}^2\,\Omega\xi(\cosh^2\Omega\xi - 1)\sin(n\bar{\Omega}\xi + \phi) \\
&-\Omega^2 \sin(n\bar{\Omega}\xi + \phi) - 2n\bar{\Omega}\Omega\,\mathrm{sech}\,\Omega\xi \sinh\Omega\xi \cos(n\bar{\Omega}\xi + \phi) - n^2\bar{\Omega}^2 \sin(n\bar{\Omega}\xi + \phi)]\mathrm{sech}\,\Omega\xi \\
&+m^2\tilde{A}\,\mathrm{sech}\,\Omega\xi \sin(n\bar{\Omega}\xi + \phi) - \tfrac{1}{4}\lambda\lambda_f^2\tilde{A}^3\,\mathrm{sech}^3\,\Omega\xi[3\sin(n\bar{\Omega}\xi + \phi) - \sin 3(n\bar{\Omega}\xi + \phi)] \\
&= 3\lambda\tilde{A}A^2\,\mathrm{sech}^3\,\Omega\xi \sin(n\bar{\Omega}\xi + \phi).
\end{aligned} \tag{35}$$

We will ignore the terms with $\cos(n\bar{\Omega}\xi + \phi)$ and $\sin 3(n\bar{\Omega}\xi + \phi)$. The equation (35) yields

$$\tilde{A}_0 = 0 \quad \text{and} \quad \tilde{A}_{\pm} = \pm 2\lambda_f^{-1}\sqrt{\tfrac{1}{3}\lambda^{-1}(c_*^2\vartheta^2 K^2 I - \omega^2 B^2)\Omega^2 - A^2}\,. \tag{36}$$

And

$$m^2 = \tfrac{1}{2}(c_*^2\vartheta^2 K^2 I - \omega^2 B^2)(\Omega^2 - n^2\bar{\omega}^2)\,. \tag{36.1}$$

Thus, our solution can only be valid for a very weak interaction of fields Φ and f. Using (36.1) we rewrite (36) in the form

$$\tilde{A}_{\pm} = \pm 2\lambda_f^{-1}\sqrt{\tfrac{2}{3}\lambda^{-1}m^2(\Omega^2 - n^2\bar{\Omega}^2)^{-1}\Omega^2 - A^2}\,. \tag{36.2}$$

Thus, the quantum amplitude increases infinitely, if $\Omega^2 = n^2\bar{\Omega}^2$.

We assume that the expressions (34) and (36) determine quantum perturbations acting to the dynamic landscape of the scalar field. Perhaps, these expressions approximately describe the eigenfunctions of the equation (33). Let us compare these functions with the eigenfunctions which describe oscillations within different potential wells. The comparison is presented in Fig. 3 for the eigenfunctions (localized wave packets) calculated for different potential wells and different equations.

The left curves were obtained for the square potential well, the centre curves were obtained for the well having the parabolic potential well. The right wave packets were obtained for the rectangular well which models the well of the dynamic landscape of the scalar field (see Figs. 1 and 2). It was assumed that certain quantum wave packet excites the bubble oscillating on the bottom of the well. The dimension of the packet may be much larger than the dimensions of the bubble.

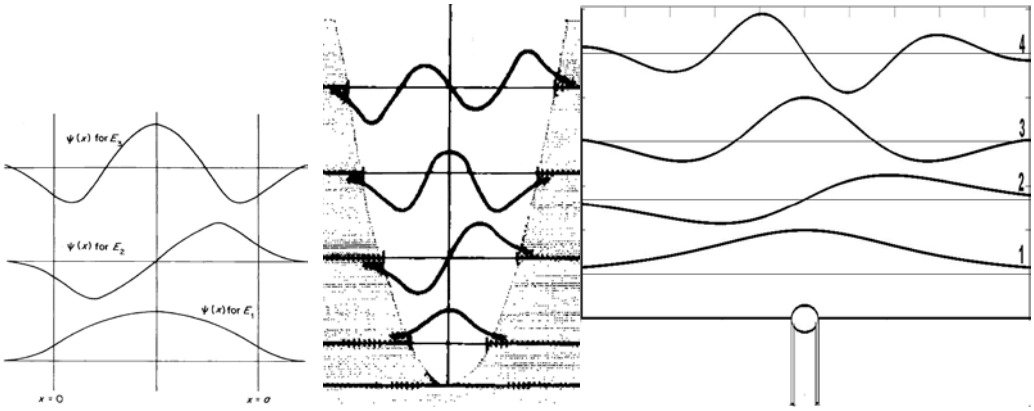

Fig. 3. The eigenfunctions calculated for different potential wells and different equations.

The eigenfunctions presented in the left part and the centre correspond to the Schrödinger equation [94]. The wave packets presented in the right part are calculated according to (34) for different $n\bar{\Omega}$ and ϕ. Namely, the curve 1 correspond to $\operatorname{sech}\xi$, the curve 2 correspond to $\operatorname{sech}\xi\sin\xi$, the curve 3 correspond to $\operatorname{sech}\xi\cos 2\xi$ and the curve 4 correspond to $\operatorname{sech}\xi\sin 3\xi$. It is seen that these localized wave packets describe well the data of the Schrödinger equation.

Indeed, it is known that some wave equations can describe wide spectra of physical phenomena. In the next subsection we illustrate this assertion additionally.

Conclusion. The expressions (34) and (36) determine quantum perturbations acting on the bubbles of energy oscillating on the bottom of the potential wells (see, additionally, Fig. 1 and 2 describing the dynamic landscape of the scalar field and its potential). These wave packets may be considered as external perturbations (sources) acting on the bubbles. In this case the equation (14.1) is rewritten in the form:

$$\tfrac{1}{2}(\omega^2 B^2 - c_*^2 \vartheta^2 K^2 I)\Phi_{\xi\xi} + m^2\Phi - \lambda\Phi^3 = f(\xi). \qquad (37)$$

We assume that this equation determines possibility of the origin of the Universe.

3.2. Oscillons and experiments

Oscillons which were shown in Figs. 1 (right) and 2 are not well known. The oscillating localized objects, similar to those presented in Figs. 1 and 2, have different names: oscillons, breathers, pulsons and Q-ball [6, 64, 65]. The name, oscillon, was introduced in [64], where spherically symmetric unstable scalar field configurations (‘bubbles’), were examined.

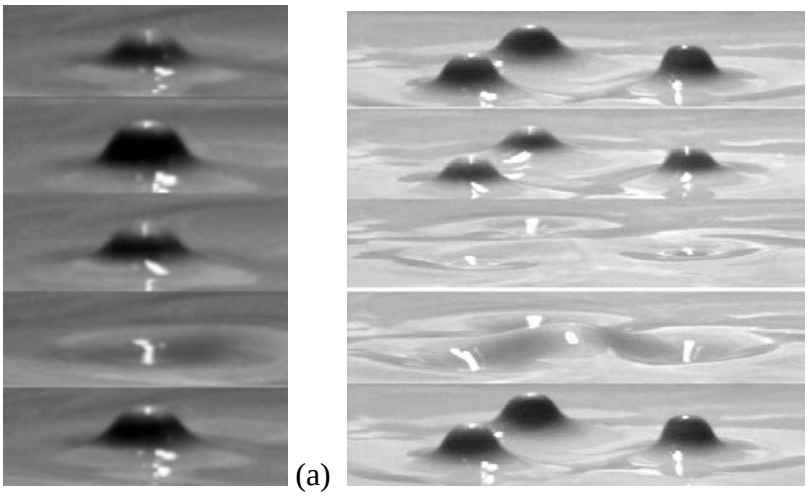

(a) (b)

Fig. 4. Typical oscillons excited on a suspension surface. One oscillon (a) and three oscillons (b) [66].

Oscillons on a granular layer were observed in 1996 [65]. Then oscillons were excited on suspension layers [66]. The photos illustrating the last case are presented in Fig. 4.

In the experimental system [66] a layer of a suspension was vibrated vertically. A cubical container with 20 cm sides was used, with Plexiglas lateral boundaries. The container was mounted on a mechanical shaker providing vertical acceleration from 0 to 30 *g*. The range of driving frequencies was limited from 10 to 60 Hz. The maximum amplitude was 1.25 cm. The working suspensions were a mixture of water with commercial clay powder. At a critical value of acceleration the initial spatially-uniform surface loses its stability, and localized vertically-oscillating waves (oscillons) can appear (Fig. 4).

On a granular layer, strongly-localized vertically-vibrating waves can also occur. Examples of such waves arising on a layer of small balls are shown in Fig. 5.

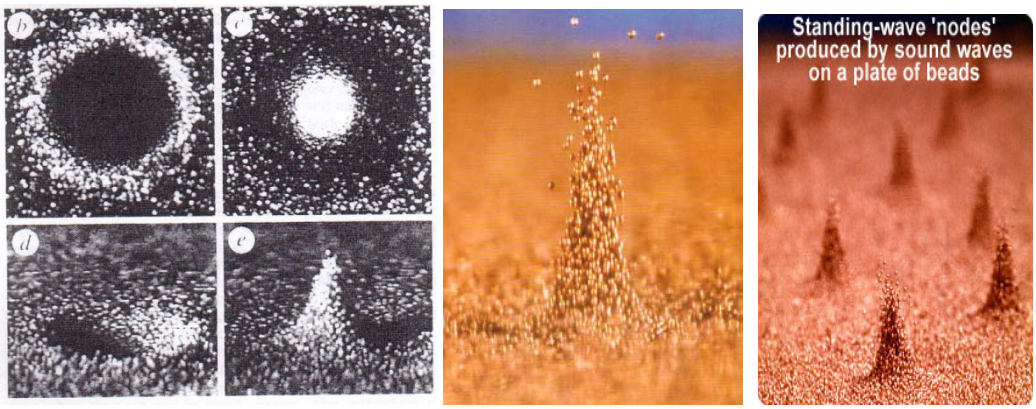

Fig. 5. Periodical granular column and crater on the surface of a vertically-excited layer: b and c are a bird view, d and e, are a side view [65]. A granular column and two craters near it, and granular standing-wave ‘nodes’ [67].

The oscillon is an axisymmetric excitation. It oscillates with half the frequency of the exciting frequency. It is a parametrically-excited localized wave. During one cycle of the excitation it is a peak; on the next cycle it is a crater. The oscillon may be started by touching the surface of brass balls with a pencil. After formation of the surface crater, the oscillon begins to bounce up and down, while the surrounding material stays in the same place. The oscillon height is usually larger than the layer thickness (Fig. 5). Thus, these excitations may be considered as strongly-nonlinear waves, where the vertical motion of the particles is connected with their horizontal motion. Similar spatiotemporally oscillating localized nonlinear waves having properties of both standing and travelling waves were described in [68-74]. In particular, the analytical theory of these waves was developed.

A possibility of the existence of space oscillons in the very early Universe immediately after the end of the inflationary stage of its expansion was found [73, 75-78]. It is very important for us that those oscillons were described by the solutions of NKGE. Thus, the similar objects were found in different strongly nonlinear wave systems. The similarity is not surprising since it is well known that a nonlinear wave equation often describes different experimental results. Therefore, we can expect that the solutions (19) and (34) also describe different experimental results, for example, for the Bose-Einstein condensate (BEC).

BEC was obtained for the first time in 1995 year. Then the study of its properties began. Some of them were explained by strongly nonlinear properties of BEC [79]. In particular, localized regions of periodic oscillations were found in the condensate (Fig. 6).

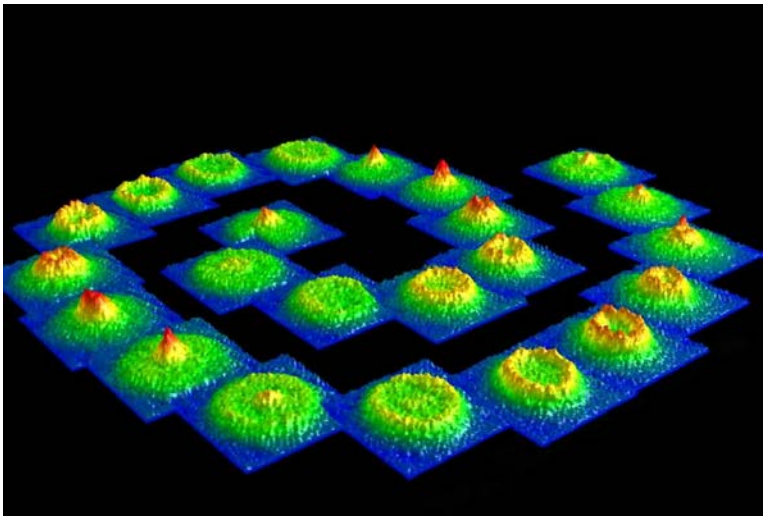

Fig. 6. Oscillations of a rotating Bose-Einstein condensate [80].

It is interesting that it was shown in 2001 that the local oscillons similar to those found in BEC can exist in the cosmic space [81].

Modeling of oscillons in the Bose-Einstein condensate (BEC). In Fig. 7 we present data of calculations of the landscape of the scalar field which simulate the Bose-Einstein condensate oscillations.

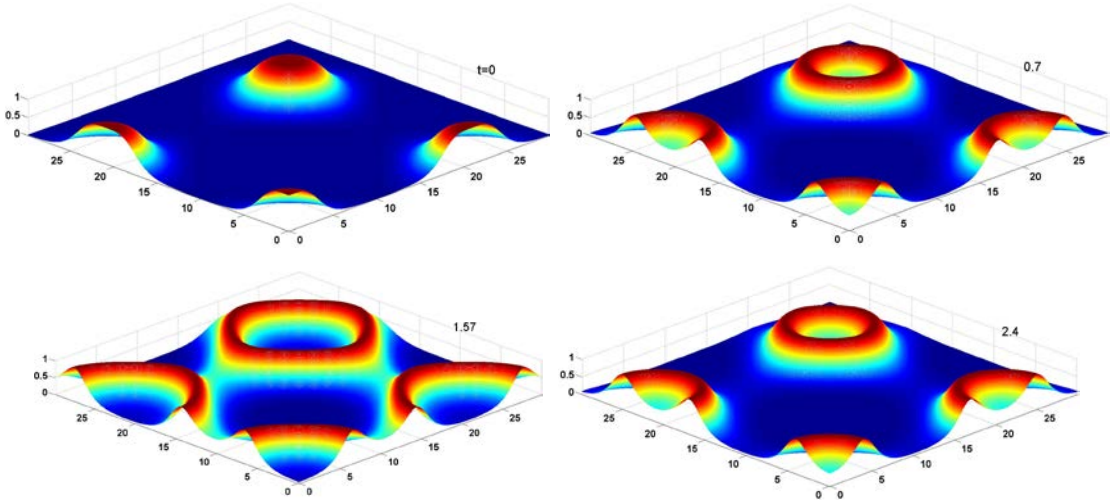

Fig. 7. Radially oscillating rings are shown which form the peak during the convergence. The data simulate the experiments with the Bose-Einstein condensate [80] (see, also, http://www.lkb.ens.fr/recherche/atfroids/anglais/vortex_an.html) .

It is assumed that $R^* = 0.001$, B =3.5, $\omega = 1$, $K = 5$ and $\vartheta = 0.15$. We stress that in contrast with Fig. 1 we have assumed $K = 5$ in Fig. 7. As a result, unlike Fig. 1 the thickness of the rings in Fig. 7 increased. Fig. 7 begins to remind data of the experiments with the Bose-Einstein condensate (Fig. 6).

Thus, there are a certain similarity between the oscillations of the dynamic part of the scalar field (Fig. 7) and the data from the experiments studying the wave processes in the Bose-Einstein condensate (Fig. 6).

Simulation of oscillons on surfaces of granular and liquid media. Oscillons on the surfaces of these media are usually parametrically-excited localized standing waves. Generally speaking, they remind the oscillons presented in Figs. 6 and 7. However, here, as it is shown in Fig. 8, the oscilons form peaks and craters in two different places during the full period of the oscillations.

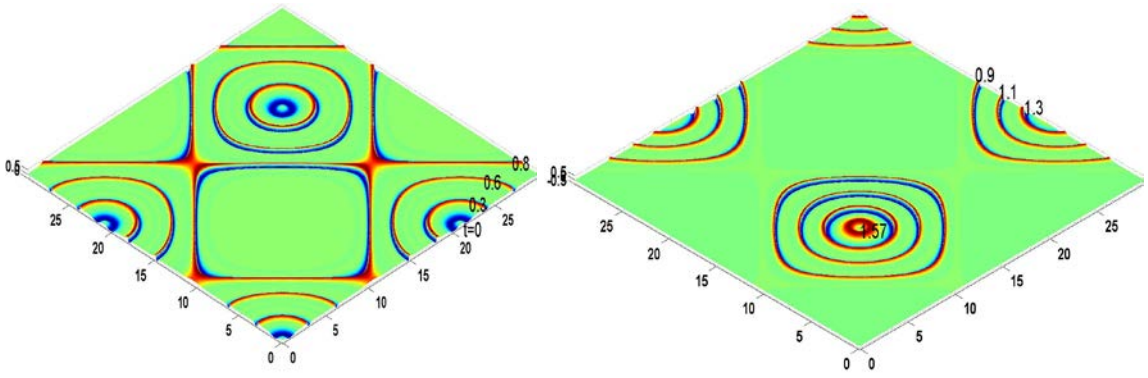

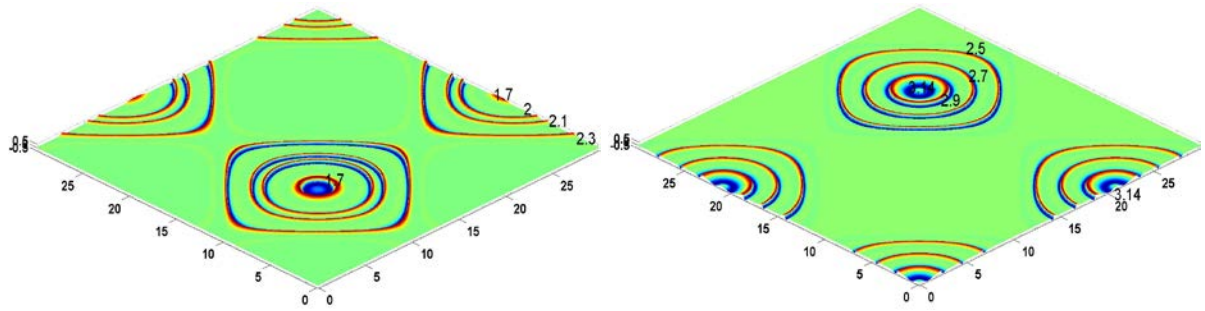

Fig. 8. Landscapes calculated according to the expression $\operatorname{sech}\xi \sin\frac{1}{2}\xi$ (34) for t = 0.3; 0.6; 0.8; 0.9; 1.1; 1.3; 1.57; 1.7; 2; 2.1; 2.3; 2.5; 2.7; 2.9; 3.14.

The results of the calculations are presented in Fig. 8 for different moments of time. It is assumed, that $R^* = 0$, B =150, $\omega = 1$, $K = 75$, $\vartheta = 0.15$, $n\bar{\omega}$=0.5 and φ=0. First the craters appear when t =0 (Fig. 8). Then the craters begin to expand. Their depth decreases (t = 0.3; 0.6; 0.8). After that each crater changes its position (t = 0.9; 1.1; 1.3; 1.57) and starts to convert into a peak (a top of a hill, t =1.57). These peaks rapidly transform into the craters. Then the process of the expansion of the craters repeats (t = 1.7; 2; 2.1; 2.3), but at new locations. The craters begin to move to the old locations if approximately t = 2.35. After that they begin to increase the depth (t = 2.5; 2.7; 2.9; 3.14). After t = 3.14 the described process is repeated.

Oscillons are usually modeled with the help of numerical calculations [65, 75-78]. However, we have shown that they may be also studied analytically in the context of the theory of extreme waves [58-60, 68-74].

3.3. Simple model of the origin of the Universe: mathematics and imaginations

We considered the structures of the landscapes of the scalar field and scalar potential. Generally speaking, the amplitudes of these reliefs may be quite different. This fact is very important for our research since the origin of the Universe may be imagined as an eruption of the scalar field from some potential well. But how deep may these wells be and how intensive may the fields be ? The replies are determined by the constants m^2 and λ.

For example, if $\lambda = 10^{-15}$ we have for different m^2 the following expressions for coefficients $\lambda^{-1}m^4$ and $\sqrt{2}\lambda^{-0.5}m$ which determine the potential well (32) and the scalar field (29).

1. Let $m^2 = 10^{-2}$, then $\lambda^{-1}m^4 \approx 10^{11}$ and $\sqrt{2}\lambda^{-0.5}m \approx 10^{6.5}$. In this case apparently the field cannot erupt from the potential well;
2. Let $m^2 = 10^{-5}$ then $\lambda^{-1}m^4 \approx 10^{5}$ and $\sqrt{2}\lambda^{-0.5}m \approx 10^{5}$. In this case apparently the field can erupt from the potential well;

3. Let $m^2 = 10^{-7}$ then $\lambda^{-1}m^4 \approx 10$ and $\sqrt{2}\lambda^{-0.5}m \approx 10^4$. In this case the field erupts out of the potential well.

We also stress that the depth of the potential well is determined by the difference $[(\operatorname{sech}\eta + \operatorname{sech}\xi)^2 - (\operatorname{sech}\eta + \operatorname{sech}\xi)^4]$ (32), which may be very small in contrast with $\operatorname{sech}\xi$ (29), which determines the scalar field.

All this determines that after the jump the value of the scalar field can greatly exceed the depth of the potential well. If this takes place, the field can erupt out of the pre-universe. Then it can form the Universe.

The solutions of the subsection 2.2 demonstrate the possibility of jumps of the scalar field in the point where $\eta = \xi$. As a result, the field obtains the great positive value. Of course the landscape of the scalar field is changed at the moments of the jump. Different landscapes illustrating this change are shown in Fig. 9.

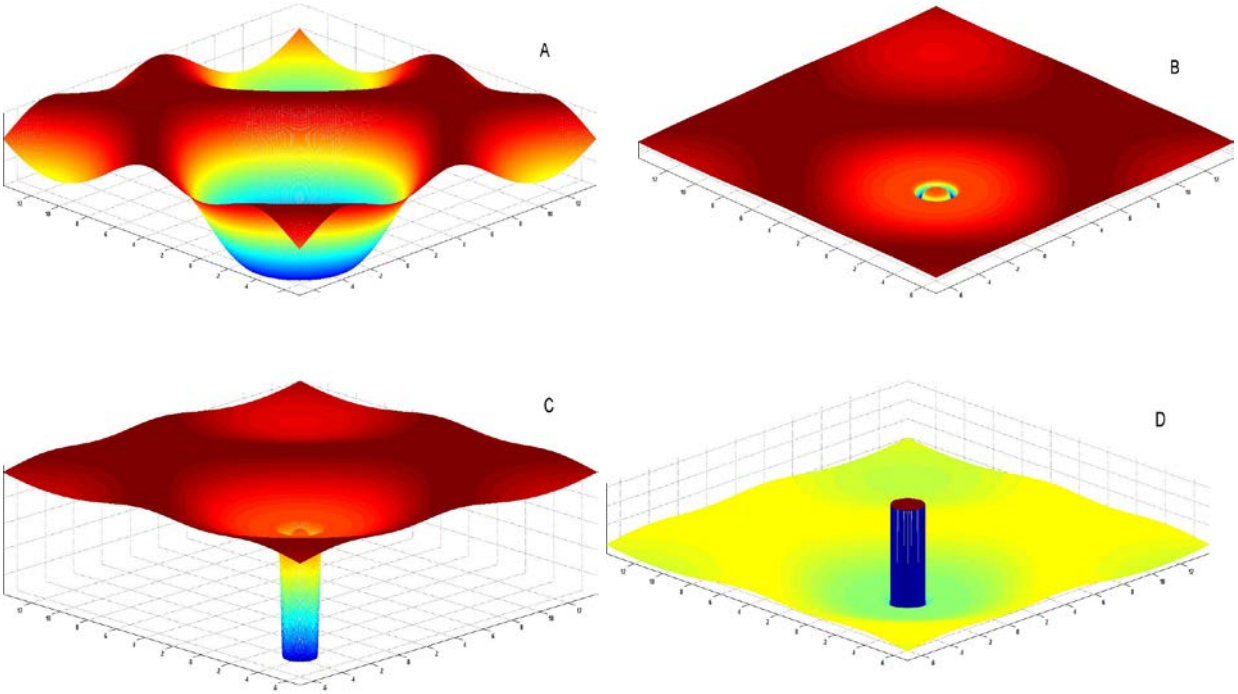

Fig. 9. The rough scheme of the jump. A sequence of pictures of the scalar potential (A) and the scalar potential plus the scalar field (B, C, D). The pictures demonstrate the landscapes before the jump (A, B, C) and the results of the jump (D).

The picture A shows the element of the landscape of the static potential. The pictures B and C shows the sum of the static potential and the dynamic part of the scalar field at same moment of time. The scalar field is located in the valley of the potential. The picture B is the bird's-eye view, the picture C is the side

view. The picture D is the bird's- eye view on the landscape after the jump of the scalar field. We think that the local jump of the landscape (Fig. 9) illustrates well the main results of the subsection 2.2. We stress that the local variation of the landscape which is presented in Fig. 9 is very instant and may be extremely large. We illustrate the main result of Fig. 9 by Figs. 10-12.

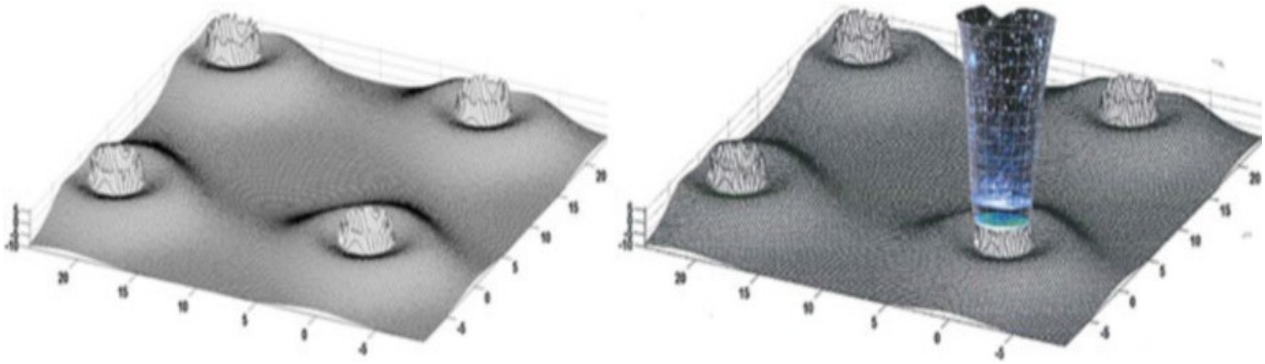

Fig. 10. The rough scheme of the development of the scalar field into the Universe. The two-dimensional landscape of the pre-universe (left) and the scheme of the origin of the Universe (right) [59].

Fig. 10 (right) shows qualitatively results of quantum perturbations, bifurcations and resonances [59]. On the other hand, it corresponds qualitatively to the jump of a bubble of the scalar field to a new, very high energy level. The birth of our Universe can put in compliance with this jump of the bubble.
Fig. 11 [90] illustrates additionally this point of view.

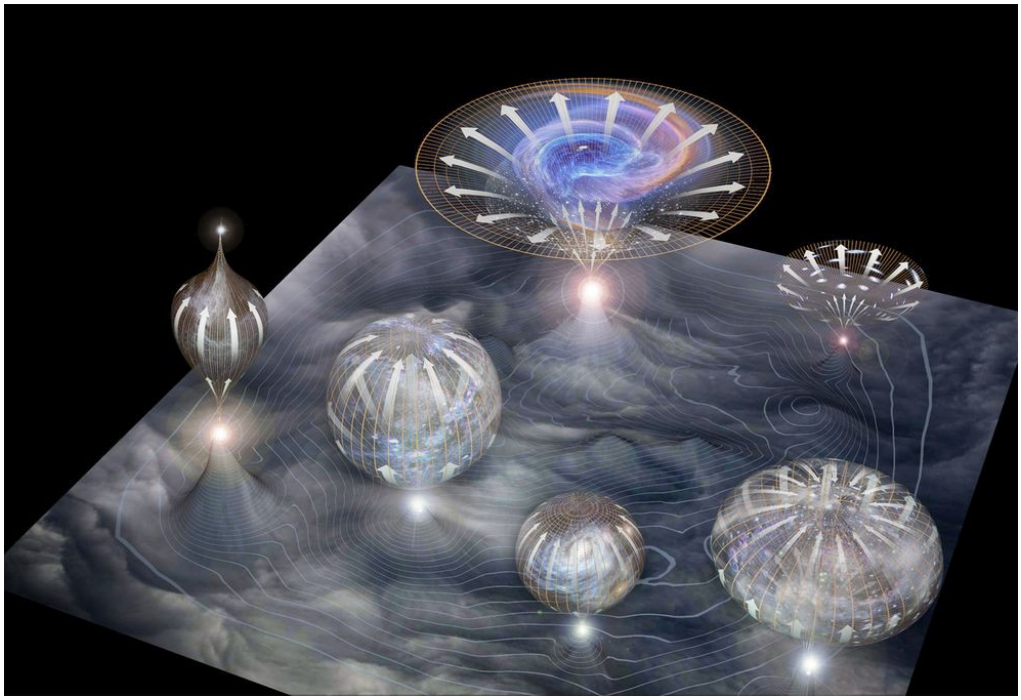

Fig.11. Image credit: Moonrunner Design, via http://news.nationalgeographic.com/news/2014/03/140318-multiverse-inflation-big-bang-science-space/.

At the same time there is certain analogy of the result of Fig. 9 with an eruption of a volcano. This analogy is supported by Fig. 12.

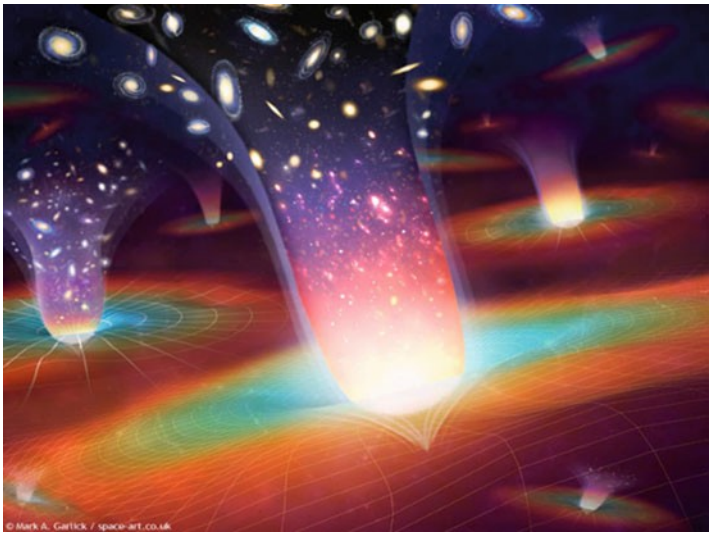

Fig. 12. A rough scheme of the eruption of universes from the potential wells of a pre-universe [91].

Of course, pictures like Figs. 11 and 12 may be considered as some wild speculations connected with unsolved problems of science. Indeed, some cosmological theories may be considered as crazy. The society should get the habit of them. The pictures like Figs. 11 and 12 should help to understand the crazy ideas better. On the other hand the scientific art which were showed in the last figures, could popularize scientific ideas and results which are not supported up to this moment by experiments and observations [41, 42, 47, 48, 92, 93].

Remark. We recall that basic laws of quantum mechanics is applicable for our analysis. In particular, it is well known [41, 61] that the energy density and the energy pressure of the scalar field depend on derivatives $\Phi_i^{\,2}$, $\Phi_t^{\,2}$ and the scalar potential $V(\Phi)$. Thus, these density and pressure can increase infinitely in the points of discontinuity. Due to above circumstances, our Universe can emerge having practically infinite energy and mass.

4. Modeling of instant quantum actions

We have the solutions describing many dynamic scalar fields. Our interpretation of the above results is

that the spacetime of the pre-universe is pervaded by a number of scalar fields. It is possible to assume that they correspond to some boson-like fields. The fields are localized in same space, which is determined by coordinate ξ. All fields focus at the same place where they could interact. As a result the external sources may appear in the field equations. The simplest version of the similar equation has a form $(-\Box+\mu^2)G(x,y)=\delta(x,y)-(3/8\pi^2)H^4$. This equation was used by Hawking [21]. Similar equations take into account the quantum effects.

We assumed that the quantum perturbations exist in the potential well of pre-universe (the subsection 3.1) . We also found that these perturbations, developing within the scalar field, act on certain bubble located in the bottom of the well. In this case the equation describing the periodical oscillations of the bubbles should supplement with the term which takes into account these perturbations.

4.1. Theoretical model

Using the results of the subsection 3.1 we will consider the equation (14.1) subject to an instant external quantum action. As a result an new term appears in the right-hand side of the equation [82]. In this case we have

$$\tfrac{1}{2}(\omega^2B^2-c_*^2\vartheta^2K^2I)\Phi_{\xi\xi}+m^2\Phi-\lambda\Phi^3=\varphi(\Phi)\tilde{A}\delta(\overline{\xi})\,. \tag{38}$$

Here $\overline{\xi}$ is a point subject to the quantum action, $\delta(\overline{\xi})$ is the Dirac delta function (the impulse function), $\tilde{A}$ is the amplitude of the quantum fluctuation and $\varphi(\Phi)$ is an arbitrary function. Let

$$\Phi=A\operatorname{sech}\xi \text{ and } \varphi(\Phi)=\operatorname{sech}^2\overline{\xi}\sinh\overline{\xi}\,. \tag{39}$$

We will consider the field in the vicinity of $\overline{\xi}$. It is assumed that there the value of the field can change discontinuously as a result of the quantum kick (fluctuation). This discontinuous change in the field is computed by integration (38) from $\xi_j=\overline{\xi}-\varepsilon$ to $\xi_{j+1}=\overline{\xi}+\varepsilon$:

$$\begin{aligned}&\tfrac{1}{2}(\omega^2B^2-c_*^2\vartheta^2K^2I)[\Phi_\xi(\overline{\xi}+\varepsilon)-\Phi_\xi(\overline{\xi}-\varepsilon)]\\&+\int_{\overline{\xi}-\varepsilon}^{\overline{\xi}+\varepsilon}(m^2A\operatorname{sech}\xi-\lambda A^3\operatorname{sech}^3\xi)d\xi=\tilde{A}\int_{\overline{\xi}-\varepsilon}^{\overline{\xi}+\varepsilon}\varphi(\Phi)\delta(\overline{\xi})d\xi.\end{aligned}$$

This equation is rewritten using (39). As a result we have

$$\begin{aligned}
&\tfrac{1}{2}(\omega^2 B^2 - c_*^2 \vartheta^2 K^2 I)[-(A\,\mathrm{sech}^2\,\xi \sinh\xi)_{\bar{\xi}+\varepsilon} + (A\,\mathrm{sech}^2\,\xi \sinh\xi)_{\bar{\xi}-\varepsilon}] \\
&+2m^2[(A \arg\tan(\exp\xi))_{\bar{\xi}+\varepsilon} - (A \arg\tan(\exp\xi))_{\bar{\xi}-\varepsilon}] \\
&-\tfrac{1}{2}\lambda[(A^3\,\mathrm{sech}^2\,\xi \sinh\xi)_{\bar{\xi}+\varepsilon} - (A^3\,\mathrm{sech}^2\,\xi \sinh\xi)_{\bar{\xi}-\varepsilon}] \\
&-\lambda[(A^3 \arg\tan(\exp\xi))_{\bar{\xi}+\varepsilon} - (A^3 \arg\tan(\exp\xi))_{\bar{\xi}-\varepsilon}] = \tilde{A}\int_{\bar{\xi}-\varepsilon}^{\bar{\xi}+\varepsilon} \mathrm{sech}^2\,\bar{\xi} \sinh\bar{\xi}\,\delta(\bar{\xi})d\xi.
\end{aligned} \tag{40}$$

Let $\varepsilon \to 0$ and $(A)_{\bar{\xi}+\varepsilon} >> (A)_{\bar{\xi}-\varepsilon}$. First we collect the terms with

$$(\mathrm{sech}^2\,\xi \sinh\xi)_{\bar{\xi}+\varepsilon}. \tag{41}$$

As a result we have an equation linking $A_{\bar{\xi}}$ and $\tilde{A}$,

$$A_{\bar{\xi}}{}^3 + \lambda^{-1}(\omega^2 B^2 - c_*^2 \vartheta^2 K^2 I) A_{\bar{\xi}} + 2\tilde{A}\lambda^{-1} = 0. \tag{42}$$

Then we collect the terms with

$$\arg\tan(\exp\xi)_{\bar{\xi}+\varepsilon} \tag{43}$$

In this case the equation (40) approximately yields that

$$m^2 = \tfrac{1}{2}\lambda(A_{\bar{\xi}})^2. \tag{44}$$

Thus, we have the algebraic equation (42) coupling the nonlinear properties of the field, the amplitude of the quantum action and coefficient $\omega^2 B^2 - c_*^2 \vartheta^2 K^2 I$. If $\tilde{A} = 0$, then (42) yields the former solutions (22), (24) for the dynamic part of the field. However, for some values of $\tilde{A}$ a solution of (42) can be larger $A_+ = \sqrt{2}\lambda^{-0.5} m$ (24). In this case, the vicinity of the point $\bar{\xi}$ can erupt out of the potential well. On the other hand, the equation (42) can have discontinuous solutions. Of course, the discontinuous solutions are only for certain values of the coefficient $\omega^2 B^2 - c_*^2 \vartheta^2 K^2 I$ and $\tilde{A}$, λ^{-1}. Let us consider conditions determining an origin of the discontinuous solutions.

4.2. Calculations and their analysis

Our aim in this section to study an influence of $\omega^2 B^2 - c_*^2 \vartheta^2 K^2 I$ and $\tilde{A}$ on solutions of the equation (42). Effects of λ^{-1} is also analysed, but for the most calculations we use $\lambda = 10^{-15}$ [41].

4.2.1. Discontinuous jump of the scalar field

We remind that ϑ, B, ω and K in (42) are arbitrary values which determine the coefficient $\omega^2 B^2 - c_*^2 \vartheta^2 K^2 I$. This coefficient will be considered as a variable.

Discontinuous jump. The solutions of (42) are also depended strongly on effects of nonlinearity (the coefficient λ) and $\tilde{A}$. However, if $2\tilde{A}\lambda^{-1}$ is very small, the equation (42) has real solutions for practically any $\omega^2 B^2 - c_*^2 \vartheta^2 K^2 I$. Namely, one solution if $-\omega^2 B^2 + c_*^2 \vartheta^2 K^2 I < 0$ and three solutions if $-\omega^2 B^2 + c_*^2 \vartheta^2 K^2 I > 10^{-18}$ (see, as an example, Fig. 13A). The situation is different for strong enough quantum actions. In this case, we can construct discontinuous multivalued solutions of (42) having the jump (see, for example, a composite discontinuous curve consisting from segments 1, 4 and 5 or a composite discontinuous curve consisting from segments 2, 4 and 5 in Fig. 13B). These discontinuous multivalued curves (solutions) are also illustrated by the corresponding smooth segments in Fig. 13C.

Typical nonlinear picture of roots of the equation (42) is shown in Fig. 13. We assumed that $\tilde{A} = 10^{-21}$ (A) or $\tilde{A} = 10^{-19}$ (B and C). If approximately $-\omega^2 B^2 + c_*^2 \vartheta^2 K^2 I > 4 \cdot 10^{-18}$, there are three different real solutions of (42) (segments 1, 2 and 3). If approximately $-\omega^2 B^2 + c_*^2 \vartheta^2 K^2 I < 4 \cdot 10^{-18}$, the solution is determined by one curve, which is composed from the segments 4 and 5 (see Fig. 13B and C). The jump takes place approximately in the point $\omega^2 B^2 - c_*^2 \vartheta^2 K^2 I = -4 \cdot 10^{-18}$.

It is important that the jump to the positive values experiences fields having the negative amplitudes (segments 1 and 2). It is seen that values of these fields may be very different. However, during the jump, these fields coalesce, and begin to interact in such a way that they form a new field corresponding to the segments 4 and 5 ($-\omega^2 B^2 + c_*^2 \vartheta^2 K^2 I < 4 \cdot 10^{-18}$ (Fig. 13B)).

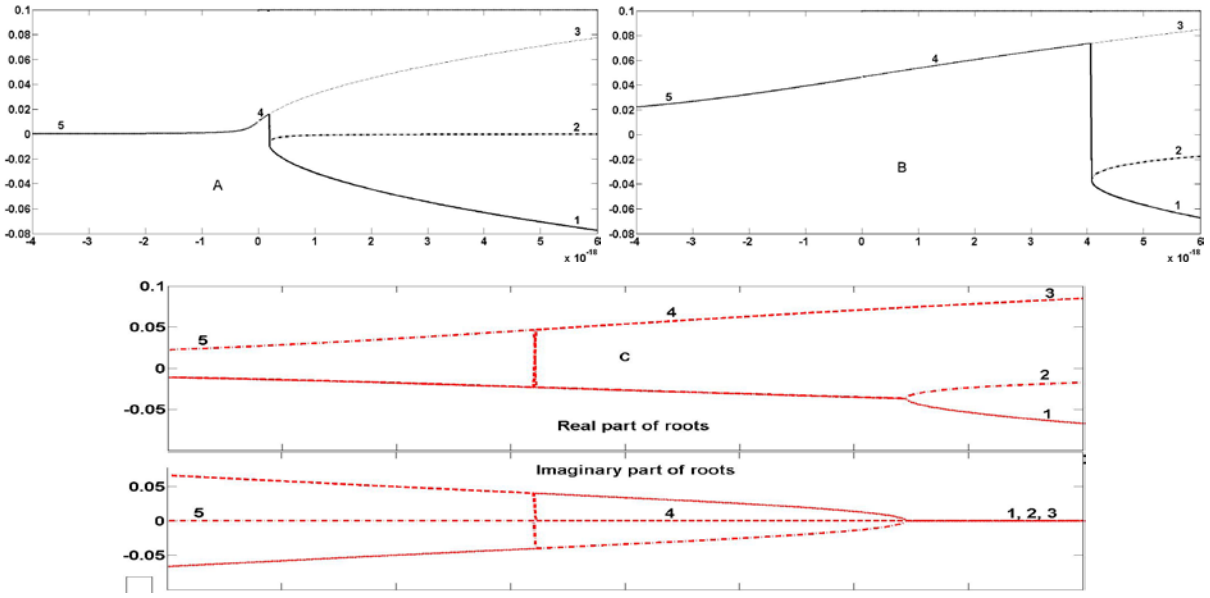

Fig. 13. Typical nonlinear picture of the amplitudes of the dynamic part calculated for $\lambda = 10^{-15}$, different values $c_*^2 \vartheta^2 K^2 I - \omega^2 B^2$, $\tilde{A} = 10^{-21}$ (A) or $\tilde{A} = 10^{-19}$ (B and C). The curves show and explain the formation of the discontinuous solutions of (42).

So we have presented in Fig. 13 the curves determining the amplitude of the function $\Phi = A\,\mathrm{sech}\,\xi$ (39) for some value ξ. Generally speaking, the equation (42) determines the amplitude A as a function of the parameters included in $\omega^2 B^2 - c_*^2 \vartheta^2 K^2 I$. These parameters link ξ with time t and coordinates x_i (6). Depending on the coefficient $\omega^2 B^2 - c_*^2 \vartheta^2 K^2 I$ the equation can define the five different segments. The segments 1, 2 and 3 correspond to three different real roots of the equation (42). We will call these real roots as A_1, A_2 and A_3. They were found for $\lambda = 10^{-15}$. In this case, we found that the weak action ($\tilde{A} = 10^{-19}$) increases instantly the amplitude of the function $\Phi = A\,\mathrm{sech}\,\xi$ up to the order of 0.1.

It is interesting to compare the results presented in Fig. 13 and the solutions (22), (24). It is seen that to a certain extent, the segment 1 (root A_1) corresponds to $A_- = -\sqrt{2}\lambda^{-0.5} m$, and the segment 2 (root A_2) corresponds to $A = 0$. The upper segment 3 (root A_3) can be compared with $A_+ = \sqrt{2}\lambda^{-0.5} m$. Of course, we do not mean 'fully compliant' speaking of the comparison, since these segments depend on the quantum action and value $\lambda^{-1}(\omega^2 B^2 - c_*^2 \vartheta^2 K^2 I)$. The latter is not equal to $-2\lambda^{-1} m^2$ (24), if there is the quantum action. Thus, comparing (22), (24), and results of Fig. 13 it can be concluded that in a case of strong enough quantum action the dynamic part of the resulting scalar field can jump and significantly exceed the maximum value $\bar{A}_+ = \sqrt{2}\lambda^{-0.5} m$ (17) for the static part of the scalar field. In this case, the dynamic part of the scalar field can leave its potential well. On the contrary, if quantum action is small enough, the dynamic part remains practically unchanged. The jump is very small or it is missing (see, as an example, Fig. 13A). In this case, the jump out of the potential well is impossible.

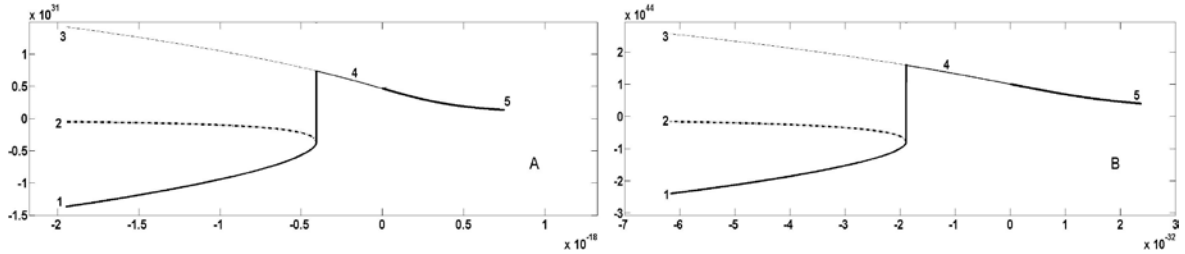

Fig. 14. Examples of extreme amplification of amplitudes of the dynamic part calculated for $\lambda = 10^{-80}$ (A) and $\lambda = 10^{-120}$ (B) when $\tilde{A} = 10^{12}$. The horizontal axis corresponds to different values of $c_*^2 \vartheta^2 K^2 I - \omega^2 B^2$. The curves show and explain the formation of the discontinuous solutions of (42).

The field amplification depends strongly on the coefficient of nonlinearity (λ). The smaller λ, the larger amplification. For example, if $\lambda = 10^{-80}$ and $\tilde{A} = 10^{12}$ then $A_{\bar{\xi}}$ is of the order of 10^{31}. If $\lambda = 10^{-120}$ and $\tilde{A} = 10^{12}$ then $A_{\bar{\xi}}$ is of the order of 10^{44} (Fig. 14).

Conclusion. We studied the influence of the nonlinearity and the amplitude $\tilde{A}$ on the size of the discontinuity (jump). According to our calculations, the field reaches the values of the order of 10^{-7}, when $2\lambda^{-1} = 10^{4}$ and $\tilde{A} = 10^{-25}$. If $2\lambda^{-1} = 10^{20}$ and $\tilde{A} = 10^{-18}$, then the jump was of order 10. If $2\lambda^{-1} = 10^{-20}$ and $\tilde{A} = 10^{-38}$, then the jump was of order 10^{-19}. Thus, the jump depends strongly on $\tilde{A}$ and λ. At the same time, we found that the jump amplification of the scalar field was proportional to $2\lambda^{-1}\tilde{A}$. For any λ^{-1} this amplification changes approximately from $10^{20}\tilde{A}$ to $10^{17}\tilde{A}$. Thus, the scalar field can be greatly amplified as a result of the weak enough quantum action.

These results are limited by the action of the instant quantum fluctuation. Let us consider more general cases of finite time quantum fluctuations.

4.2.2. Structure of the jump and its formation

We emphasize that we were talking about an instantaneous jump, which corresponds to the instantaneous quantum action. We have calculated the value of the scalar field jump for certain values of the variable $\omega^2 B^2 - c_*^2 \vartheta^2 K^2 I$, nonlinearity and the quantum fluctuation. At some spacetime point characterized by these parameters, the scalar field can jump out of the pre-universe. This jump can be viewed as a starting point of the evolution of our universe. Of course, this point requires a careful study.

It is noted in [58-60] that the jump can have, on a closer examination, a complex structure. It may consist of a series of jumps. The jumps from one energy level to another level can be accompanied by the destruction of the spacetime and the appearance of particles of matter and energy.

We now focus on multiple jumps of the scalar field. First we look closer at the jump area in Fig. 13. To do this, we assume that in this area there is a resonant dependence of the amplitude $\tilde{A}$ (42) on the parameters ω, B, ϑ and K of the bubble oscillations. Thus, we assume that the amplitude of the quantum action $\tilde{A}$ can vary with $\omega^2 B^2 - c_*^2 \vartheta^2 K^2 I$. This is a strongly localized resonant variation, therefore the field remains at the point $\bar{\xi}$.

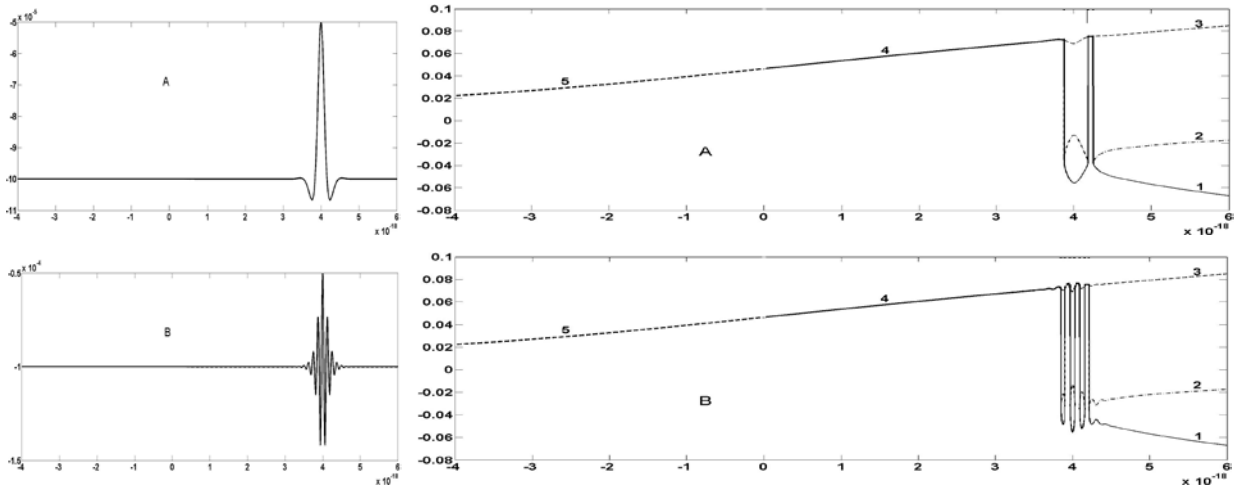

Fig. 15. Two examples of discontinuous oscillations of the scalar field. The quantum actions are shown on the left. The horizontal axis corresponds to different values of $c_*^2\vartheta^2K^2I-\omega^2B^2$.

Some results of the calculations are presented in Fig. 15. We assumed that

$$\lambda^{-1}\tilde{A}=0.5\cdot10^{-4}[-1+0.5\mathrm{sech}(0.01z)\cos(\gamma z)]. \tag{45}$$

Here $z=4000+(\omega^2B^2-c_*^2\vartheta^2K^2I)\cdot10^{21}$, $\tilde{A}\approx10^{-19}$, γ is a constant and $\lambda=10^{-15}$. The curves of Fig. 15A are calculated for $\gamma=0.01$. The curves of Fig. 15B are calculated for $\gamma=0.05$. It is seen from Fig. 15 that the weak action ($\tilde{A}\approx10^{-19}$) increases the amplitude of the function $\Phi=A\,\mathrm{sech}\,\xi$ (39) up to the order of 0.1. In contrast with Fig. 13 we now have multiple jumps.

Of course, the number and size of jumps (discontinuities) depend on many circumstances. Generally speaking, they can appear in different points of the horizontal axis. This case is illustrated by Fig. 16. We assumed for calculations that

$$\lambda^{-1}\tilde{A}=\gamma\cdot10^{-19}[-1-0.5\mathrm{sech}(0.01z)\cos(0.01z)]. \tag{46}$$

Here $z=5000+(\omega^2B^2-c_*^2\vartheta^2K^2I)\cdot10^{21}$, $\tilde{A}\approx10^{-25}$, γ is a constant and $\lambda=10^{-4}$. The curves of Fig. 16A are calculated for γ=1.425. The curves of Fig. 16B are calculated for γ=1.4375.

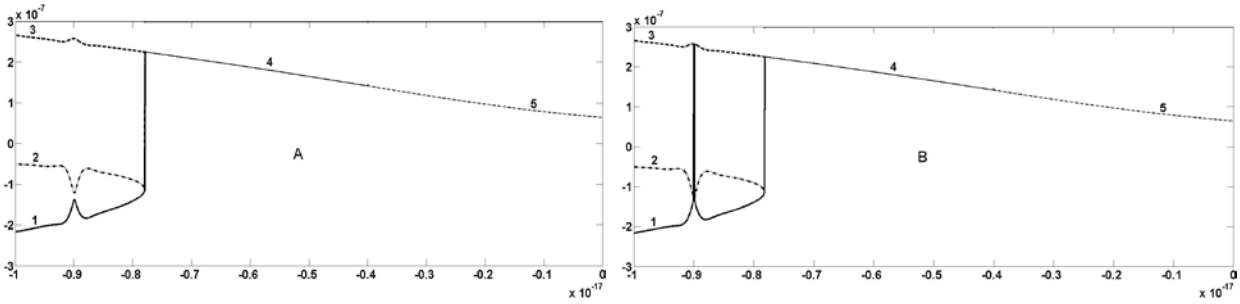

Fig.16. An example of the formation of the jump (discontinuity) which can eject the piece of the scalar field out of the pre-universe into the new spacetime [58-60]. The horizontal axis corresponds to different values of $\omega^2 B^2 - c_*^2 \vartheta^2 K^2 I$.

The appearance and location of the jumps depend strongly on the amplitude of the quantum fluctuation $\tilde{A}$ and λ. Small enough quantum action can locally change the amplitudes of the field, but cannot form the new jump (Fig. 16 A). The jump forms if the quantum amplitude increases enough (Fig. 16 B).

We can have an extremely large amplification of the scalar field due to the jump. According to our calculations the scalar fields of the bubble jump to approximately same value **(**$\approx 10^{18}\tilde{A}$): both the inner part of the bubble (the curve 2 (the zero-like field)) and its surface (the curve 1 (the negative field)). It seems if there is a sufficiently strong quantum action, then the scalar field can jump out of the potential well.

5. Finite time quantum actions

Figs. 13-16 show the possibility of a very strong change in the amplitude of the dynamic part. It opens a possibility for the energy bubble to jump out instantly of the potential well. However, generally speaking, this phenomenon may be not instantaneous. It is determined by the quantum fluctuations (see the subsection (3.1)). For example, if the quantum fluctuation is determined as $f(\xi) = \tilde{A}\operatorname{sech}\Omega\xi$ (the curve 1 in Fig. 3), the equation (37) yields

$$\tfrac{1}{2}(\omega^2 B^2 - c_*^2 \vartheta^2 K^2 I)\Phi_{\xi\xi} + m^2\Phi - \lambda\Phi^3 = \tilde{A}\operatorname{sech}\Omega\xi\,. \tag{47}$$

Since $\operatorname{sech}\Omega\xi \approx \operatorname{sech}^3\Omega\xi$, we rewrite (47) in the form

$$\tfrac{1}{2}(\omega^2 B^2 - c_*^2 \vartheta^2 K^2 I)\Phi_{\xi\xi} + m^2\Phi - \lambda\Phi^3 = \tilde{A}\operatorname{sech}^3\Omega\xi\,. \tag{48}$$

Let $\Phi = A\operatorname{sech}\Omega\xi$. In this case the equation (48) yields the equation for the amplitude A,

$$\lambda A^3 + (\omega^2 B^2 - c_*^2 \vartheta^2 K^2 I)A + \tilde{A} = 0. \tag{49}$$

It is easily seen that this equation practically coincides with the equation (42) for the instant quantum action. Therefore all results obtained for the last case are valid for the quantum fluctuation $\tilde{A}\operatorname{sech}\Omega\xi$.

5.1. 'Short' quantum actions

We have examined the effects of the instant and extremely short quantum actions on the scalar field and obtained the results linking directly nonlinearity of the scalar field and the emergence of the Universe. In particular, the instant and finite duration quantum actions are described by similar equations (see the equations (42) and (49)). Their solutions have a bifurcation at the point where $\omega^2 B^2 \approx c_*^2 \vartheta^2 K^2 I$ (Fig. 13A). Now we consider the bifurcation point more attentively using the equation (37) and the expression (34) which determines the quantum action. Equation (37) is greatly simplified near $\omega^2 B^2 \approx c_*^2 \vartheta^2 K^2 I$. Let us examine the continuous and discontinuous solutions of the equation near this point in order to further investigate the effect of the nonlinearity and its influence on the origin of the Universe. For this case the scalar field and the quantum action will be described by the equation

$$\Phi^3 + \bar{R}\Phi = \lambda^{-1} f(\xi). \tag{50}$$

Here $\bar{R} = -\lambda^{-1} m^2$ [58-60], $f(\xi)$ describes the quantum action. Below several examples of the quantum action are presented.

1. At first we consider a soliton-like quantum fluctuation when $\lambda^{-1} f(\xi) = \tilde{A}\,\mathrm{sech}\,\Omega\xi$ in (50) (see Fig. 17). This case corresponds to the wave packet 1, which is shown in Fig. 3. Let the parameters of the quantum fluctuation be: $\tilde{A} = -E \cdot 10^{-30}$, $\Omega = 5 \cdot 10^{29}$. For this case the solutions of the equation (50) are shown in Fig. 17 for the different E.

According to Fig. 17 the three independent fields (curves 1, 2 and 3) are described by (50) if the amplitude of the quantum action is small enough (E <0.385). The fields begin to interact and form a new composite field when the quantum action increases. In particular, the composite discontinuous solution appears when E = 0.385. In this case, the curves 1 and 2 coincide near the point zero and jump to the curve 3. As a result, the complex composite field is formed if $E \geq 0.385$. The composite solutions (pictures $E = 0.5$, 10) describe the discontinuous slope of the hill-like scalar fields and the strong amplification of the fields 1 and 2. They can reach the hill top of the composite scalar field. Then the composite scalar field reduces.

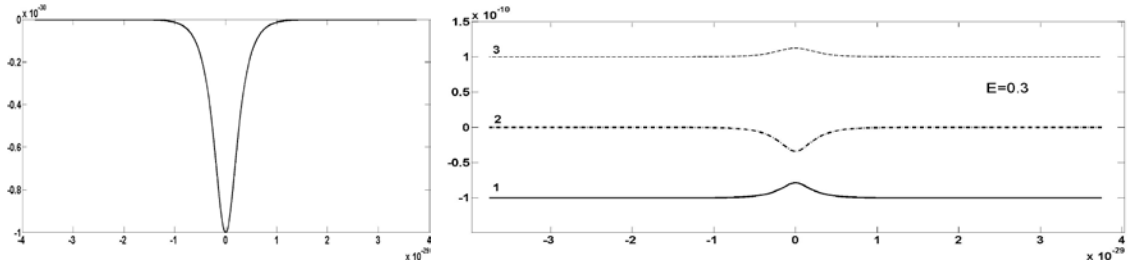

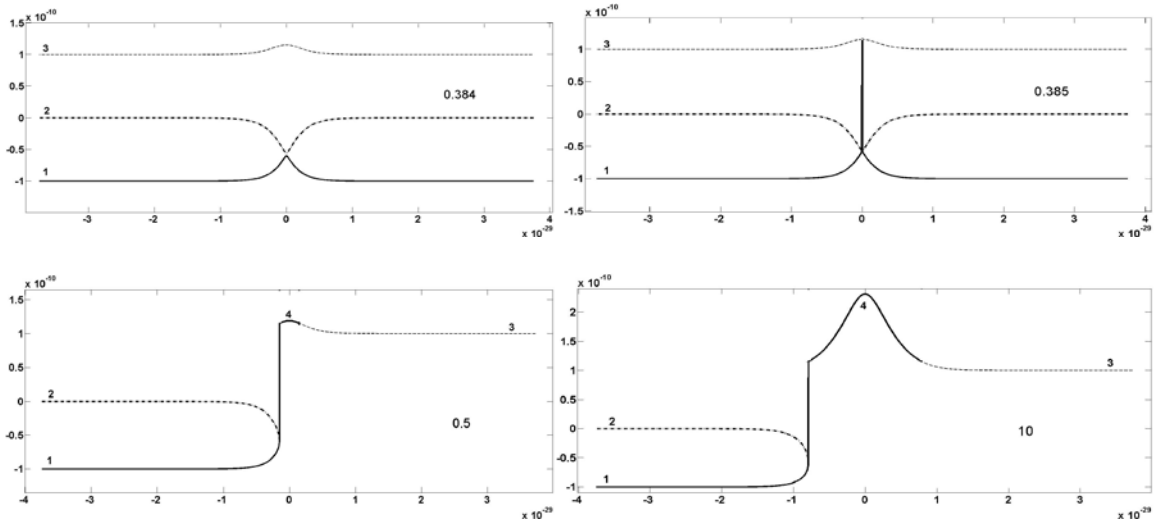

Fig. 17. Continuous and discontinuous curves described by the solutions of (50), where $\bar{R} = -10^{-20}$. The curves 1, 2 , 3 and 4 are determined by different roots of the equation. Pictures E =0.3 and E=0.384 are determined by three continuous solutions. These solutions begin to interact when E =0.385. The pictures E =0.385, 0.5 and 10 are determined by discontinuous solutions. The quantum fluctuation is the upper picture, left.

We stress that some theories describe the initial evolution of the Universe as rolling down of the scalar field from some local maximum [50, 52]. Fig. 17 shows how the scalar field can jump to this maximum. At the same time, we do not touch here the process after the jump. We only consider here the possibility of the jump. The study of the jump and the following process are the special complex problems.

2. Now we consider a case when $\lambda^{-1} f(\xi) = \tilde{A}\,\mathrm{sech}\,\Omega\xi \sin\bar{\Omega}\xi$ in (50) (see Figs. 18 and 19). This case corresponds to the wave packet 2, which is shown in Fig. 3. In this case the quantum fluctuation changes its sign, if $\xi = 0$. Let the parameters of the quantum fluctuation be: $\tilde{A} = -E \cdot 10^{-30}$, $\Omega = 5 \cdot 10^{29}$, $\bar{\Omega} = 4 \cdot 10^{29}$ (Fig. 18 the upper picture, left). The solutions of the equation (50) are shown for the different coefficient E.

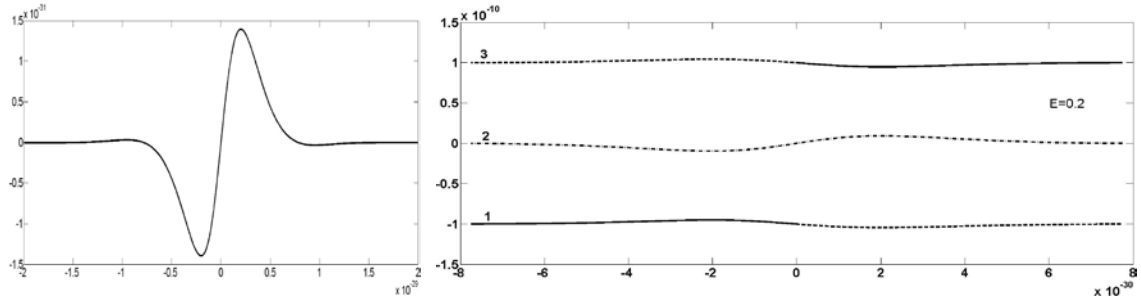

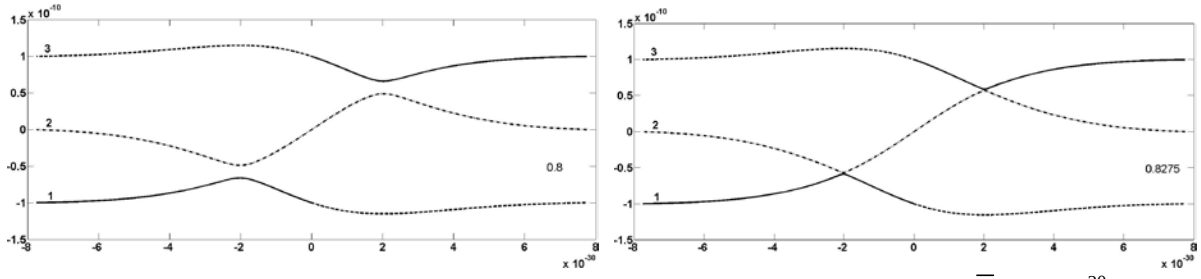

Fig. 18. Continuous curves described by the solutions of (50), where $\overline{R} = -10^{-20}$. The curves 1, 2 and 3 correspond to different roots of the equation.

The pictures of Fig. 18 are determined by three continuous solutions. If the amplitude of the action is small, then the fields are independent and the curves 1, 2 and 3 do not interact. These solutions begin to interact when E =0.8275.

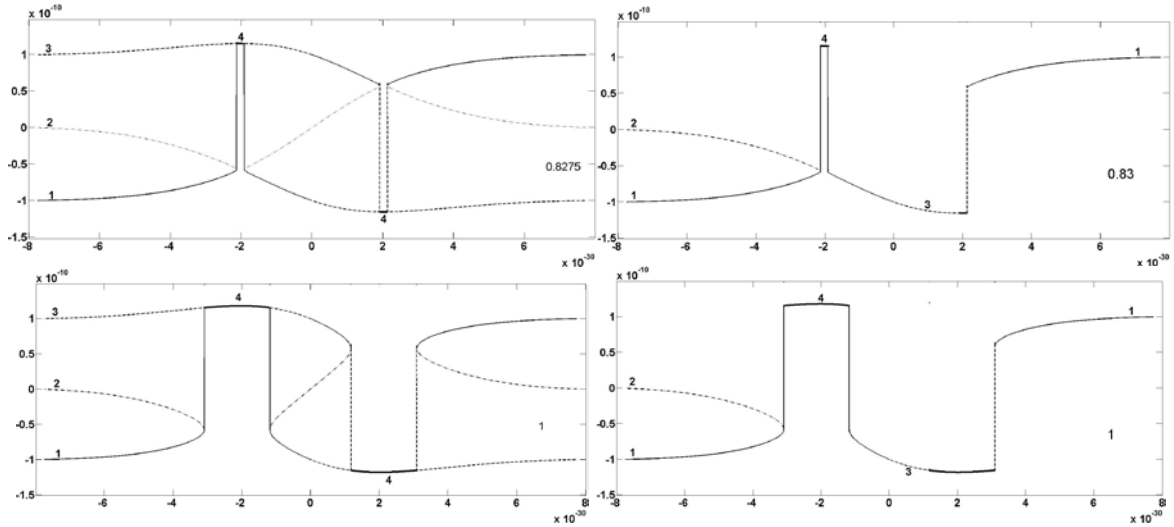

Fig. 19. Examples of the discontinuous solutions of (50) constructed for E =0.83 and E =1. The full pictures of the roots and the corresponding curves (left). The simplified pictures of the roots and the corresponding curves illustrating an appearance of the jumps and the discontinuous fields (right).

Fig. 19 shows the possibility of a very strong interaction of scalar fields determined by the equation (50), if the quantum amplitude is large enough. If E > 0.8275 then the solutions of the equation (50) are determined by the discontinuous and multivalued curves. In this case a multivalued composite discontinuous field is formed, which is determined by the discontinuous oscillations (the local jumps). These jumps determine a new fast varying scalar field.

We will study the discontinuous oscillations of the field additionally in the following subsections.

5.2. Modulated quantum actions

We assume in the equation (50) that

$$f(\xi) = \tilde{A}\lambda \operatorname{sech}\Omega\xi \cos\bar{\Omega}\xi, \tag{51}$$

where Ω and $\bar{\Omega}$ are constants. This case corresponds to the wave packet 3, which is shown in Fig. 3. The equation (50) yields

$$\Phi^3 + \bar{R}\Phi = \tilde{A}\operatorname{sech}\Omega\xi \cos\bar{\Omega}\xi. \tag{52}$$

Thus, the quantum action is being described by the packet of oscillations. We expect that the amplitude and the form of oscillations of the dynamic part can be amplified strongly inside the potential well as a result of the quantum action (51). On the other hand, we found that the amplification is possible only for certain resonant values $\bar{R} = -\lambda^{-1}m^2$ [58-60]. Below several examples of the action are presented.

1. Let the parameters of the quantum fluctuation (51) be: $\tilde{A} = 10^{-21}$, $\Omega = 5\cdot 10^{39}$ and $\bar{\Omega} = 5\cdot 10^{40}$ (Fig. 20).

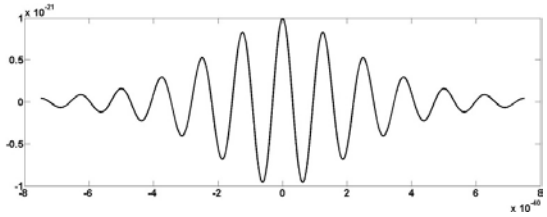

Fig. 20. The quantum fluctuation as a soliton-like packet of waves (51) [58-60].

Let $\bar{R} = -10^{-14}$. For this case the solutions of the equation (52) are shown in Fig. 21.

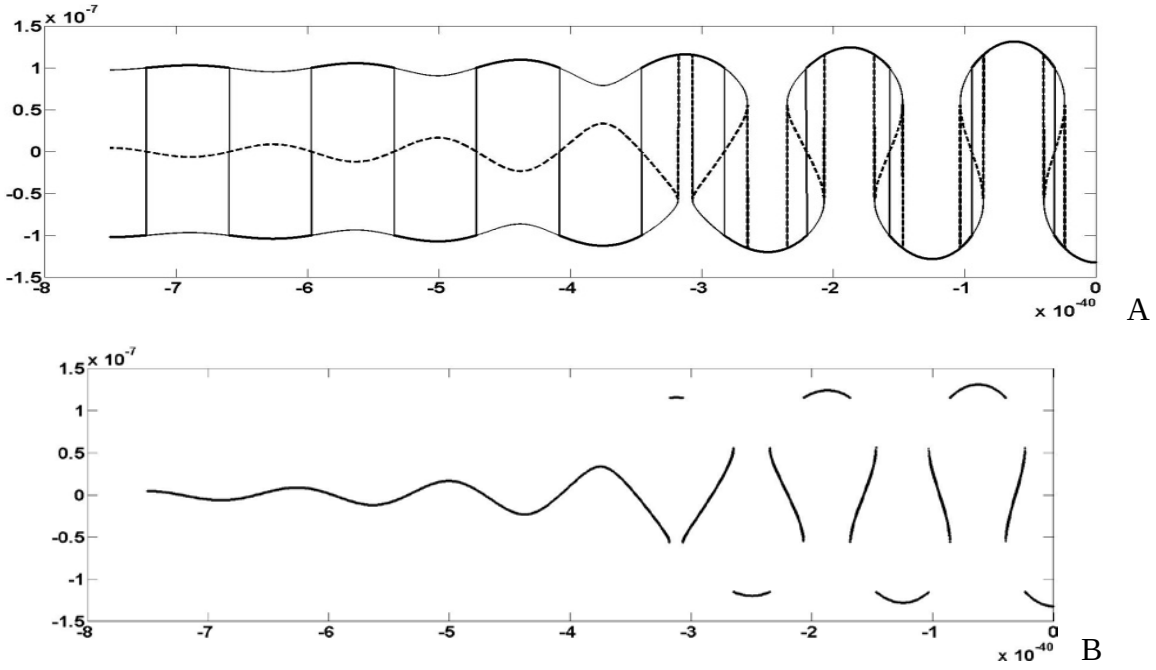

Fig. 21. The evolution of the scalar fields at the resonance ($\bar{R} = -\lambda^{-1}m^2 = -10^{-14}$) [58-60].

The curves of the picture A are determined by three types of the roots of the equation (52). These curves slightly oscillate when the horizontal coordinate is smaller than $-4\cdot10^{-40}$. In this case the curves correspond to three independent fields. The upper curve corresponds to the positive field, the middle curve corresponds to the zero field and the bottom curve corresponds to the negative field (see the subsections 2.2 and 4.2.1). These curves (fields) begin to interact when the horizontal coordinate increases more than $-4\cdot10^{-40}$. The composite (multivalued) field is formed by elements of the independent fields.

Thus, the three independent fields are described by the equation (52), if the amplitude of the quantum action is small enough (see Figs. 20 and 21 together). The fields begin to interact when the quantum oscillations increase. As a result the very complex composite field is formed. The corresponding roots (the solutions) form the profile which reminds the mushroom-like waves. We have violent nonlinear distortions of the initial scalar field and, apparently, violent nonlinear distortions of the initial spacetime. The curves B (Fig. 21) are determined by a sole type of the roots of the equation (52). These roots slightly oscillate relatively the zero line when the horizontal coordinate is smaller than $-4\cdot10^{-40}$. The curve is ruptured and strongly different pieces of the scalar field are formed, when the amplitude of the quantum action increases.

The same behaviour is observed in the following two cases, where we consider a quantum fluctuation with another parameters.

2. Let the parameters of the quantum fluctuation be: $\tilde{A}=3\cdot10^{-39}$, $\Omega=5\cdot10^{39}$ and $\bar{\Omega}=5\cdot10^{40}$.

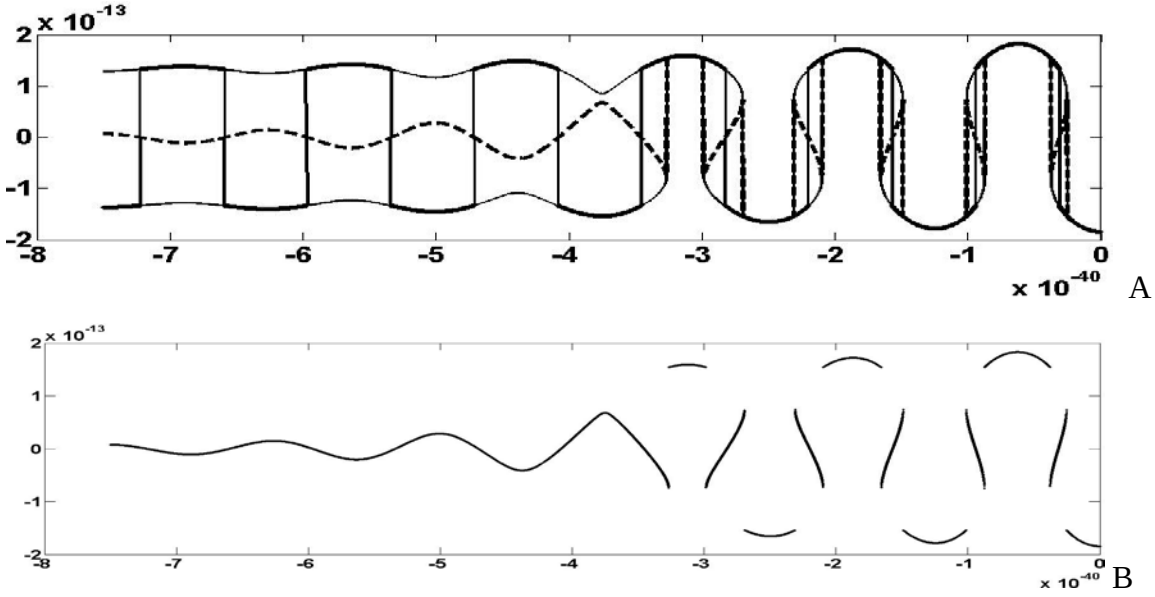

Fig. 22. The evolution of the scalar fields at the resonance ($\bar{R}=-\lambda^{-1}m^2=-10^{-25.75}$) [58-60]. The composite (multivalued) solution (A), the discontinuous solution (B).

In this case the resonant interaction of the fields take place, if $\bar{R} = -10^{-25.75}$ (Fig. 22). The curves (fields) begin to interact when the horizontal coordinate increases more than $-4 \cdot 10^{-40}$. The curves B (Fig. 24) are determined by a sole type of the roots of the equation (52).The rupture and the amplification of the scalar field are illustrated. We think that this figure demonstrates violent nonlinear distortions of the initial scalar field and, apparently, violent nonlinear distortions of the initial spacetime.

3. Let the parameters of the quantum fluctuation be: $\tilde{A} = 3 \cdot 10^{-51}$, $\Omega = 5 \cdot 10^{39}$ and $\bar{\Omega} = 10^{41}$. In this case the resonant condition is satisfied if $\bar{R} = -3 \times 10^{-34}$. The resulting fields are illustrated by Fig. 23.

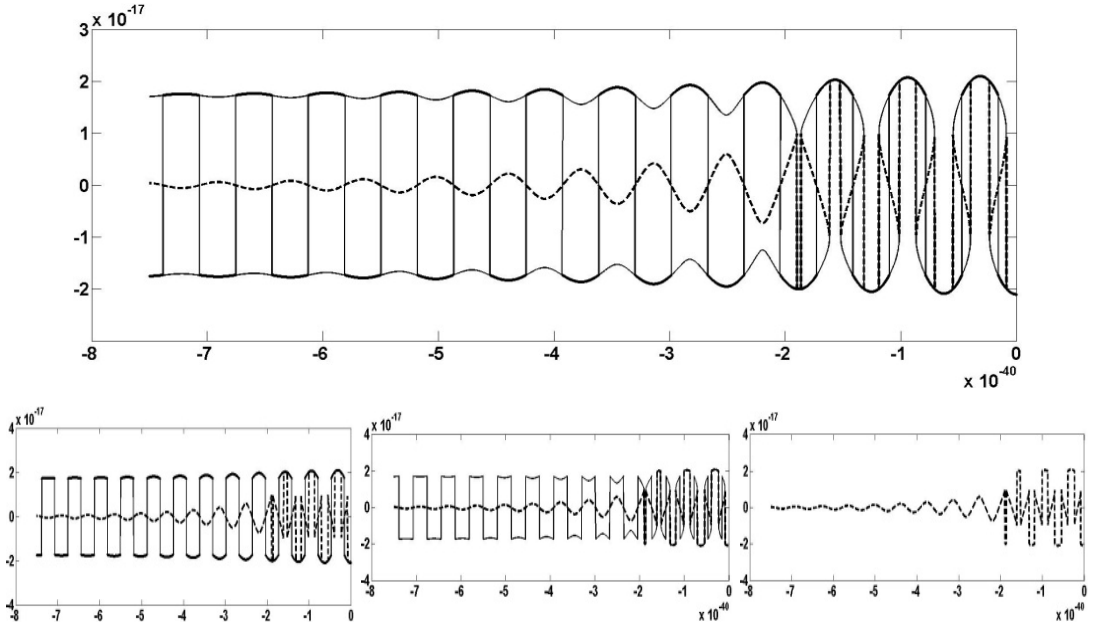

Fig. 23. The evolution of the scalar fields (solutions) during the modulated quantum action. The interaction of three fields (upper picture); the interaction of two fields (bottom pictures, left and mid); the discontinuous oscillations of one field (bottom picture, right) [58-60].

The curves Fig. 23 (bottom pictures, left and mid) are determined by two different types of the roots of the equation (52). The curve Fig. 23 (bottom picture, right)) is determined by a sole type of the roots of the equation. These curves demonstrate that quite different scalar fields might be originated due to resonant excitation of the initial scalar field by the modulated quantum actions.

In the cases considered above (Figs. 21 – 23) we found resonant parameters at which the three source independent scalar fields begin to interact and form a new composite field. The amplitude of the composite field's oscillations increases beyond that of the original fields. It may increase to a point where it becomes possible for the energy bubble to escape the potential well (Fig. 2).

The nature of the oscillations themselves change. They become very complex and can potentially contain jump discontinuities.

We found that the amplification of the fields and the strongly nonlinear evolution of their forms took place when some resonant conditions for coefficients $\bar{R} = -\lambda^{-1} m^2$ and $\tilde{A}$ of the equation (52) were satisfied. We considered cases when these resonant conditions take place. The influence of the change of the quantum fluctuations on the amplitude and the form of the resulting nonlinear scalar fields (waves) was studied.

An important result of the calculations is that a very weak quantum action can form the composite scalar field within the resonant band. Near the resonant band the field evolution may be described by tree branches of the solution. Generally speaking, the branches may interact. According to the calculations the scalar field can jump between the upper and lower branches (between positive and negative values of the energy).

Remark. The calculated results did not qualitatively change when Ω and $\bar{\Omega}$ were increased to $\Omega = 5 \cdot 10^{27}$, $\bar{\Omega} = 5 \cdot 10^{28}$.

5.3. 'Long' quantum actions

Let us study a case of the quantum fluctuations having more long duration (Fig. 24). It is assumed also that the quantum action function has a fast varying part. This part is much shorter of the action duration. Examples of similar actions are shown in Fig. 24 (centre and right).

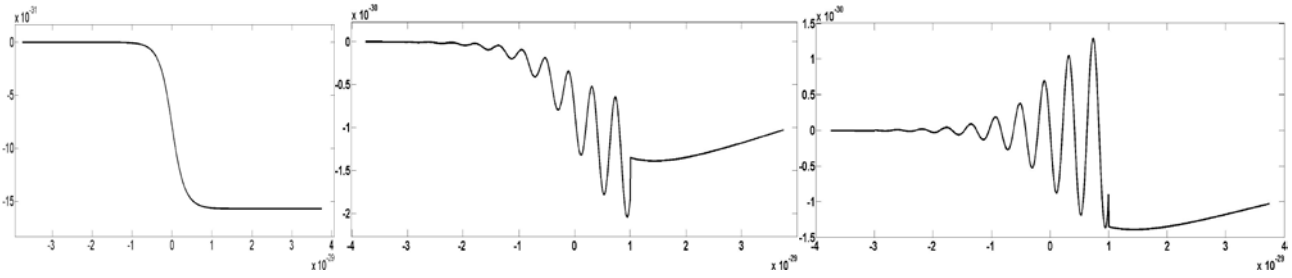

Fig. 24. The quantum action described by the expression $\lambda^{-1} f(\xi) = \tilde{A} \arg\tan[\exp(-\Omega\xi)]$ (left) and more complex curves describing the quantum action in (52) (centre and right).

The solutions of the equation (52) obtained for the above quantum actions are presented in Figs. 25-28. Considering these figures we mean that the roots 1 and 2 (the segments 1 and 2) describe the evolution of certain scalar fields 1 and 2.

1. First it is assume that $\lambda^{-1} f(\xi) = \tilde{A} \arg\tan[\exp(-\Omega\xi)]$ (Fig. 24), where $\tilde{A} = A \cdot 10^{-30}$, $\Omega = 5 \cdot 10^{29}$ and $\bar{R} = -10^{-20}$ in (52). For this case the solutions are shown in Fig. 25. It is seen that the scalar fields

are independent if A=0.01 or A=0.2 in $\tilde{A} = A \cdot 10^{-30}$. The segments (fields) 1 and 2 begin to interact when A=0.245. The jumps of the scalar fields (segments 1 and 2) to the positive values take place when A>0.246.

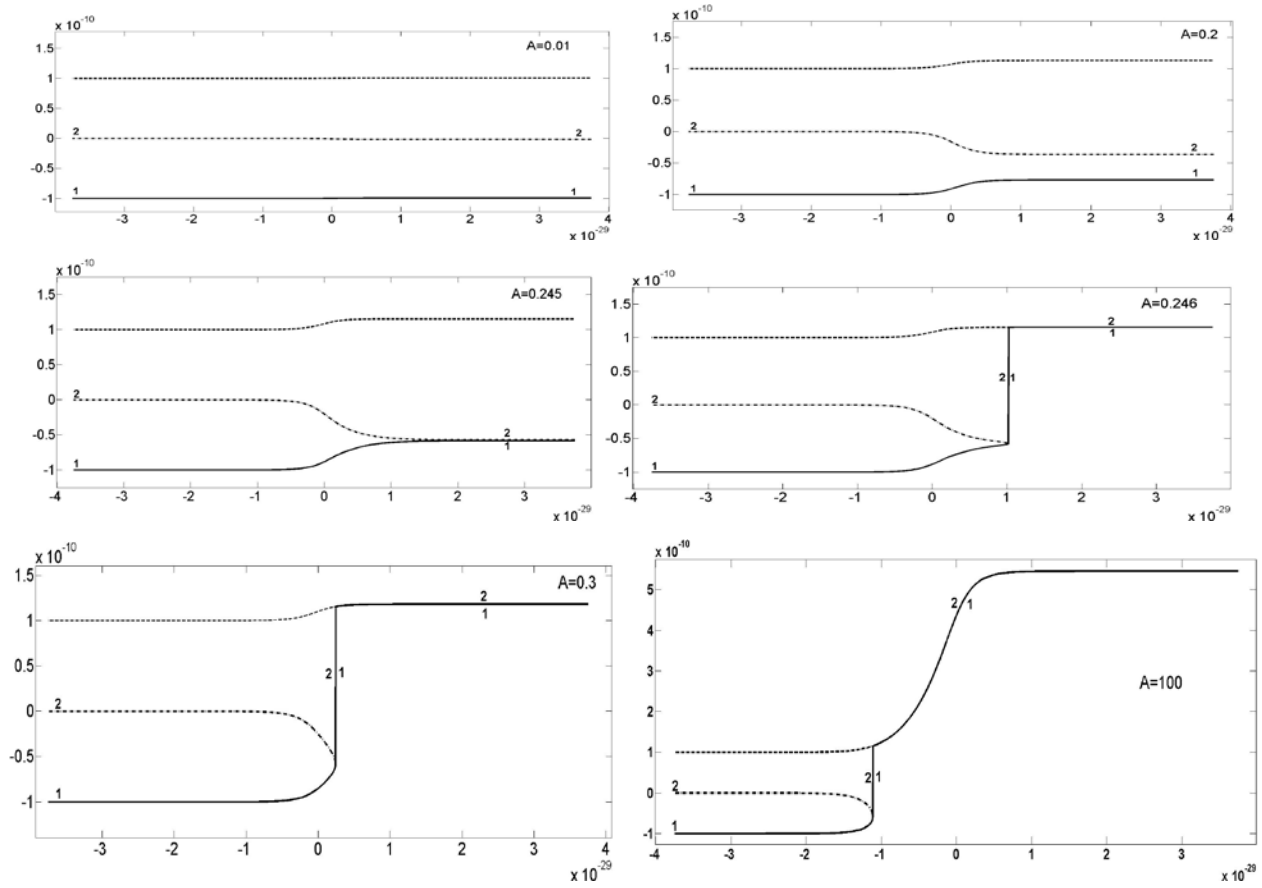

Fig. 25. Results of the quantum action $\lambda^{-1} f(\xi) = A \cdot 10^{-30} \arg\tan[\exp(-\Omega\xi)]$ (Fig. 24 left) calculated for different coefficient A. The scalar fields 1 and 2 can jump up to the top level (the plateau) if $A \geq 0.246$.

We have considered the case (Fig. 24 left) when a long quantum action is not accompanied by quantum fluctuations of small amplitude. It is known [58-60] that their impact can be very important. These fluctuations determine the possibility of the destruction of the spacetime of the pre-universe. On the other hand the small fluctuations can influence on the eruption of the scalar field from the potential well. Below we present the results of the analysis of the impact of the small fluctuations on the studied nonlinear processes.

2. Let us consider the quantum fluctuation presented in Fig. 24 (centre and right). The amplitude of the quantum fluctuation $\lambda^{-1} f(\xi)$ equals 10^{-30} and $\overline{R} = -10^{-20}$ in (52). Some results of the calculations

are presented in Fig. 26. Curves A were calculated for the action presented qualitatively in Fig. 24 (centre). Curves B were calculated for the action presented qualitatively in Fig. 24 (right).

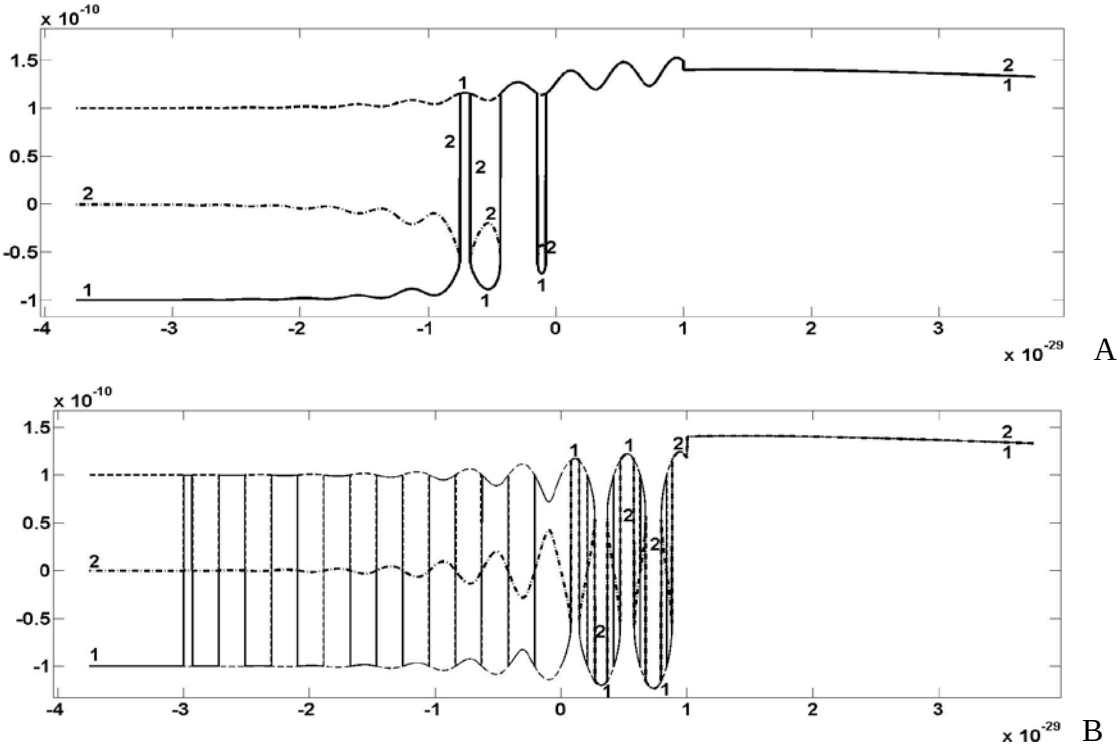

Fig. 26. Results of the quantum actions. The actions are accompanied by quantum oscillations of a small amplitude (see Fig. 24 (centre and right)).

Fig. 26 demonstrates the existence of three scalar independent fields when the horizontal coordinate is smaller -10^{-29}. These fields interact very strongly within an interval from -10^{-29} to 0 (A) and from 0 till 10^{-29} (B). The single composite field is formed after the interaction. Perhaps, this field corresponds to the origin of the Universe. The formation of the mushroom-like (elastica-like) structure [58-60] is shown in the picture B. This structure is a result of the strongly nonlinear interaction of the initially independent scalar fields.

3. The above we have considered cases when the coefficient $\bar{R}$ in (52) was very small. Now we study additionally cases when this coefficient is $\bar{R} = -10$ or $\bar{R} = -10^{20}$.

3.1. Let us consider the case of the quantum action which is similar to the case presented in Fig. 24 (centre). The calculation results are shown in Fig. 27.

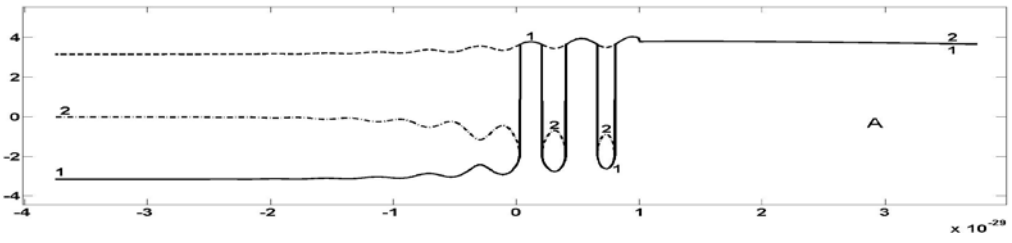

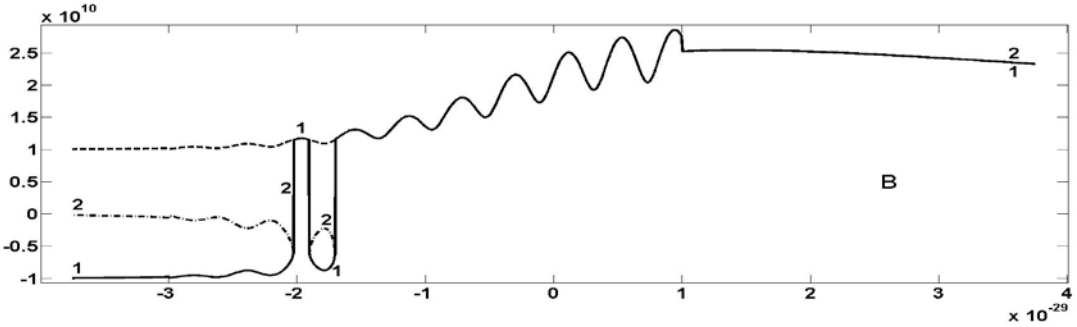

Fig. 27. Results of the quantum actions accompanied by quantum oscillations of a small amplitude.

Here the curves A are calculated for $\bar{R} = -10$ and $\lambda^{-1} f(\xi) = 10^{1.1}$. Curves B are calculated for $\bar{R} = -10^{20}$ and $\lambda^{-1} f(\xi) = 10^{31}$. In these cases we found the resonant parameters at which the three initial independent scalar fields begin to interact and form a new composite field.

3.2. Let us consider the case of the quantum action which is similar to the case presented in Fig. 24 (right). The calculation results are shown in Fig. 28.

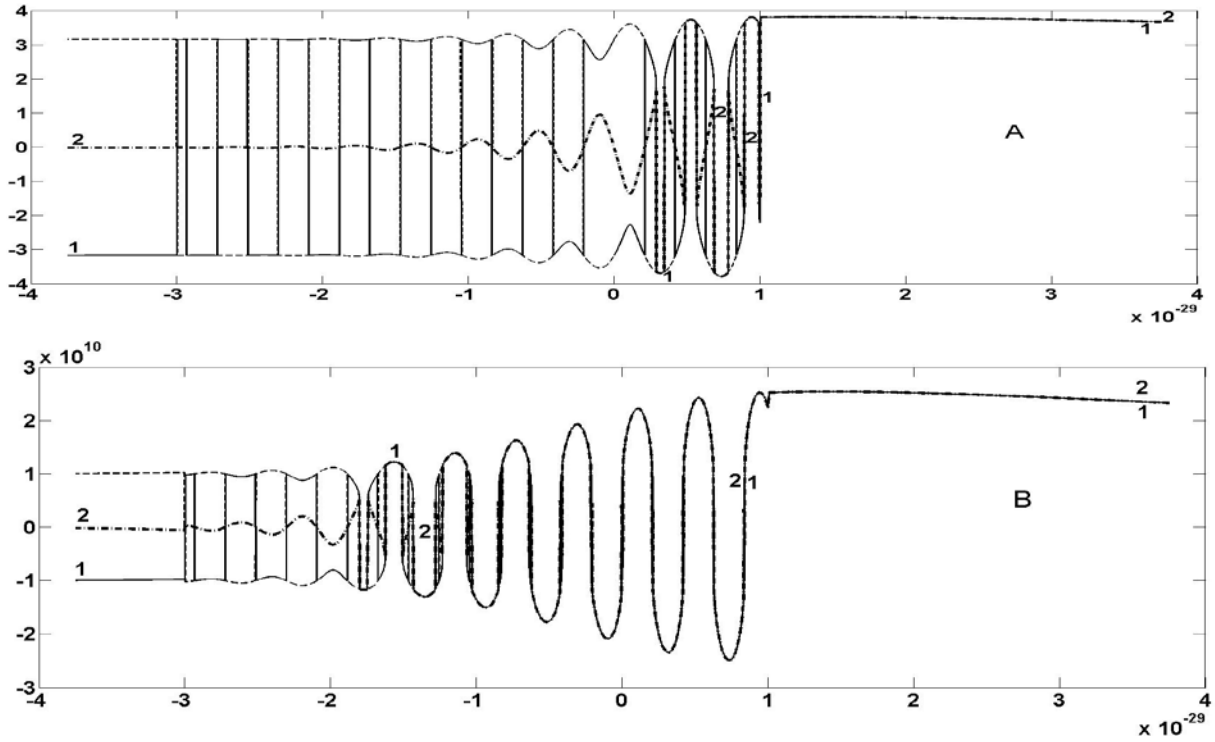

Fig. 28. Results of the quantum actions accompanied by quantum oscillations of a small amplitude. The amplitude of the quantum fluctuation $\lambda^{-1} f(\xi)$ equals -10^{-30}. The formation of the mushroom-like (elastica-like) structure [58-60] is shown.

Here the curves A are calculated for $\bar{R} = -10$ and $\lambda^{-1} f(\xi) = 10^{1.1}$. Curves B are calculated for $\bar{R} = -10^{20}$ and $\lambda^{-1} f(\xi) = 10^{31}$. We found the resonant parameters at which the three initial independent scalar fields begin to interact and form a new composite field.

Conclusion. We found the resonant parameters at which the three initially independent scalar fields begin to interact by means of multivalued discontinuous oscillations. As the result the new field is generated which is thrown on the plateau-like top of the hill (see Figs. 25-28). We think that similar new composite fields may be considered as a starting point of the evolution of the Univerve. We studied the instability of a scalar field which is caused by a quantum fluctuation. We can expect that the waves presented in Figs. 21-23 and 26-28 may be formed in different unstable systems during impact actions.

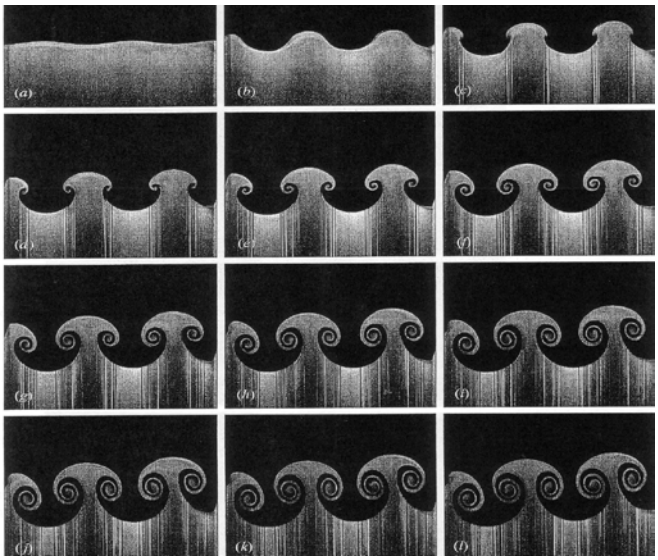

Fig. 29. An example of highly-nonlinear standing waves appearing on the interface of two liquids with different densities. The interface has the low-frequency sinusoidal perturbation [83].

Indeed, the wave forms presented in Figs. 21-23 and 26-28 are similar to the wave shapes generated due to the Richtmyer–Meshkov instability of incompressible liquids (see Fig. 29).

6. Resume of the sections 3, 4 and 5

The calculations demonstrate the existence of the distances on the horizontal coordinate line ξ, where the three scalar fields are independent from each other. On the other hand, there are the distances where the fields interact strongly. The nature of the field oscillations change. They become very complex and can contain the jump discontinuities. The composite fields are born as the result of the interaction.

The amplitude of the composite field oscillations increases beyond that of the original fields. It may increase up to a point when the energy bubble escapes the potential well. Because of the oscillations this process is described by the composite (multivalued) and discontinuous curves. We assume that noted process corresponds to the origin of the Universe [58-60].

Thus, by the way of analytic solution of the nonlinear Klein-Gordon equation we come to the initial point of some models of the origin of the Universe. In particular, the existence of some volume of the inflaton on the top of certain energetic hill is the starting point for a few inflation models [20, 50, 52].

7. The fragmentation of multidimensional spacetime during the field eruption from the potential well

We have studied the great amplification of quantum fluctuations of scalar field. In particular, the discontinuous oscillations of the fields occur. These oscillations can work as certain hammer blows smashing the local spacetime on some fundamental blocks. These blocks may differ from our ideas about the basic elements of space-time. Their sizes may depend on the energy of the oscillations (the energy of the hammer blows). In particular, it is accepted in [58-60] that spacetime may be fragmented in some one-dimensional string-like ingredients.

The multivalued and discontinuous oscillations of the composite field include the elements of the previously independent fields (see figures of sections 3 - 5). The transition of the one element to another is not necessarily smooth and continuous. The discontinuities could destroy the spacetime. The boundaries between spacetime dimensions were less stable during the eruption than they are now. As a result the multidimensional spacetime can be split into many two dimensional (space + time) elements. The spacetime fabric was transformed and fragmented when the field energy have been increased strongly. Generally speaking, it agrees with the ‘vanishing dimensions’ theory [84-87]. According this theory systems with higher energy have a smaller number of dimensions. The higher energy, the smaller spacetime dimensions. Thus, our theory implies that the number of dimensions in the Universe reduced during the eruption.

Generally speaking, the initial energy field could have many dimensions. The string theory proclaims that the number of the dimensions may be different, for example, 5, or 11 or 26. As the number of dimensions reduces, the volume of the initial bubble (clot, sphere, drop) can increase after the fragmentation very, very strongly.

The process could be visualised by imagining a three-dimensional drop of oil impacting the surface of water. As a result of the impact the oil drop is separated into many elements (particles) which spread over the two-dimensional surface of water. These elements of oil occupy in the two-dimensional space much

bigger volume than they had in the initial moment. It is important that the elements became more isolated from each other comparing to when they were inside the drop.

Qualitatively the fragmentation of the spacetime fabric could remind the atomization of the water drop (see Fig. 30). It shows the fragmentation a drop which was vibrated in the vertical direction in its fundamental axisymmetric mode [88]. The forms of the surface waves and the small drops, shown on Fig. 30, are determined by surface tension and some resonant conditions.

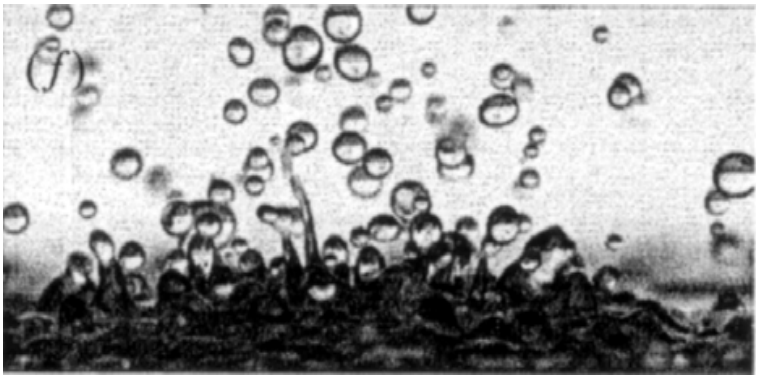

Fig. 30. Scheme of the rapid-ejection process and the formation of the cloud of particles [88].

As a result of the transresonant evolution the fragments (elements) gained the extremely high energy. Thus, in the course of the eruption the bubble (clot) of a scalar field increases strongly energy, loses the space dimensions and can strongly increase the volume. It was assumed [58-60] that the elements became absolutely isolated without any connections.

The process of fragmentation, shown in Fig. 30, can serve as a model for many natural wave phenomena [59]. In particular, as a result of the transresonant evolution of the initial field a large number of small finite elements appear which possess extremely high energy. Using the terminology of the string theory these elements may be defined as strings. They begin to vibrate (Fig. 31).

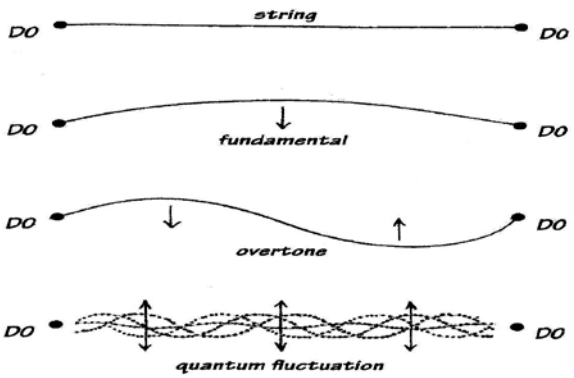

Fig. 31. Linear oscillations and a quantum fluctuation of a string stretched between two D0-branes [89].

On the whole this conclusion agrees with suggestions of Steven Carlip of the University of California, Davis [87]. In 2012 he gathered up all the theories and found that, according to many of them, the Univese had got one or two spatial dimension during the hot, dense start. In other words, geometry appears to have been radically different in the beginning. Carlip and his colleagues showed that space was split into discrete elements in the first seconds of the Universe. Each element experiences nothing outside its own existence [84-87]. Thus, the behaviour of the Universe's spacetime might be very surprising in the beginning.

8. 'Elastica'-like traveling waves: from Bernoulli, Euler and Laplace to the origin of the Universe

According to sections 3, 4, 6 and 7 it is possible to suggest that during the eruption the texture of the spacetime was fragmented in absolutely independent string-like elements. Huge kinetic energy was accumulate there. These suggestions are very similar to the base ideas of the very popular string theory [89].

Thus, the study of the origin of the Universe might be connected with analysis of strongly nonlinear oscillations of strings. It was shown that strongly nonlinear traveling waves determine similar oscillations [73, 74, 94-97]. Then the solutions describing these oscillations were applied to the problem of the origin of the Universe [58-60]. We will not concern here these solutions. It is noted only that the solutions describe well certain curves of sections 4 and 5 and the process of the birth of particles of mass and energy during the origin of the Universe [58-60].

It is important that the travelling wave solutions describes also so-called 'elastica' formers. The elastica forms attracted the attention of many of the brightest minds in the history of mathematics and physics, including James Bernoulli [100], Leonhard Euler [101], Pierre Laplace [102], Gustav Kirchhoff [103], Max Born [104] and others [98, 99]. Traditionally these forms were used for description of bending of very flexible strips, bars and strings [98, 99].

It is well know that the analysis of the deflection of a loaded strip (bar) usually begins with the Bernoulli-Euler law, according to which the bending moment at any point of the strip is proportional to the change in the curvature caused by the action of the load. In particular, James Bernoulli posed the precise problem of the elastica in 1691 [100]. Euler, building on (and crediting) the work of the Bernoullis, was the first to completely characterize the family of curves known as the elastica, and published this work as an appendix [101] in his landmark book on variational techniques. His treatment was quite definitive, and holds up well even by modern standards [98] (Fig. 32).

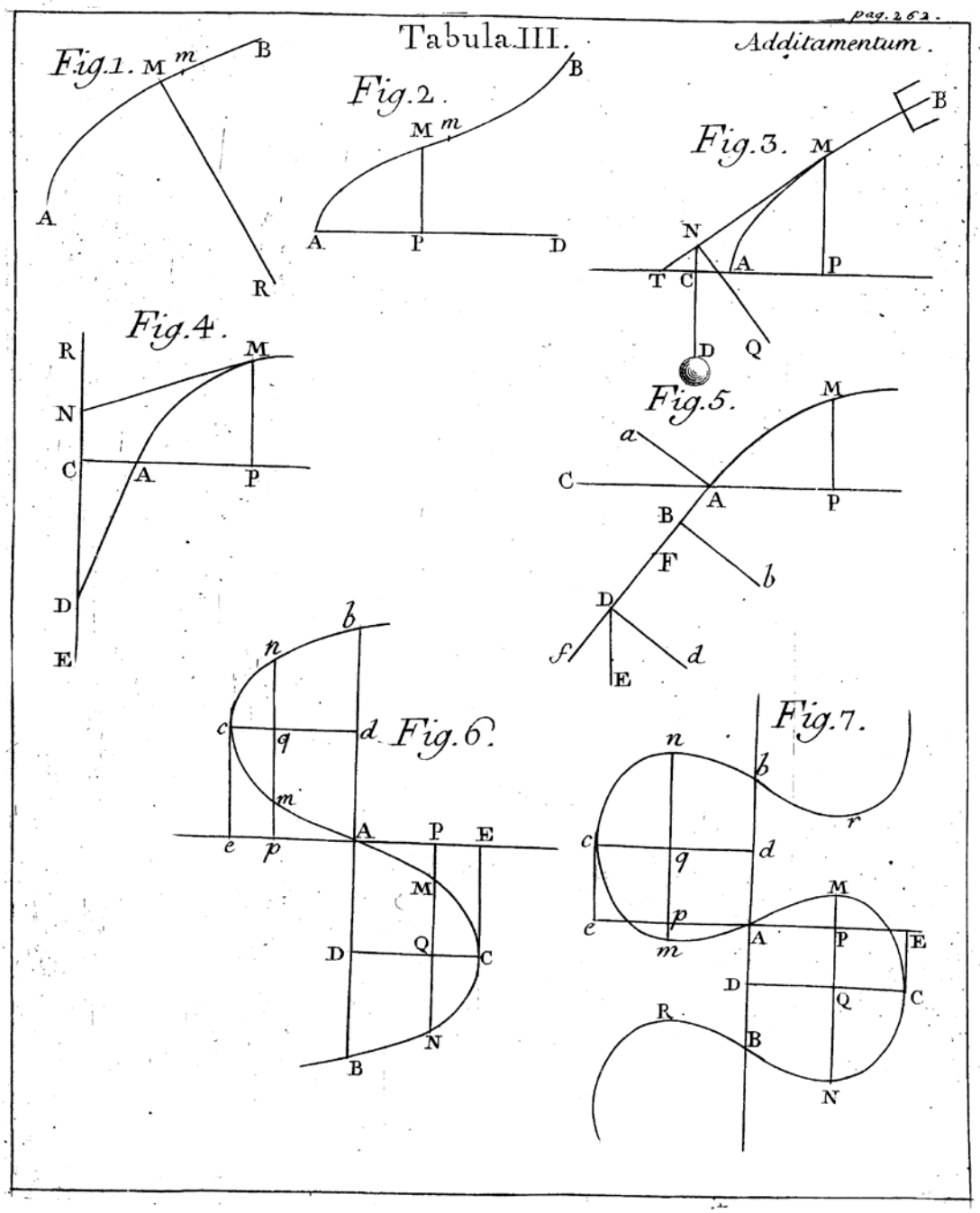

Fig. 32. Euler's elastica figures [98, 59, 101].

Euler observes that there is an infinite variety of elastic curves, but that 'it will be worth while to enumerate all the different kinds included in this class of curves. For this way not only will the character of these curves be more profoundly perceived, but also, in any case whatsoever offered, it will be possible to decide from the mere figure into what class the curve formed ought to be put. We shall also list here the different kinds of curves in the same way in which the kinds of algebraic curves included in a given order are commonly enumerated.' [101, §14]. Euler finds many curves, some of them showed in Fig. 33.

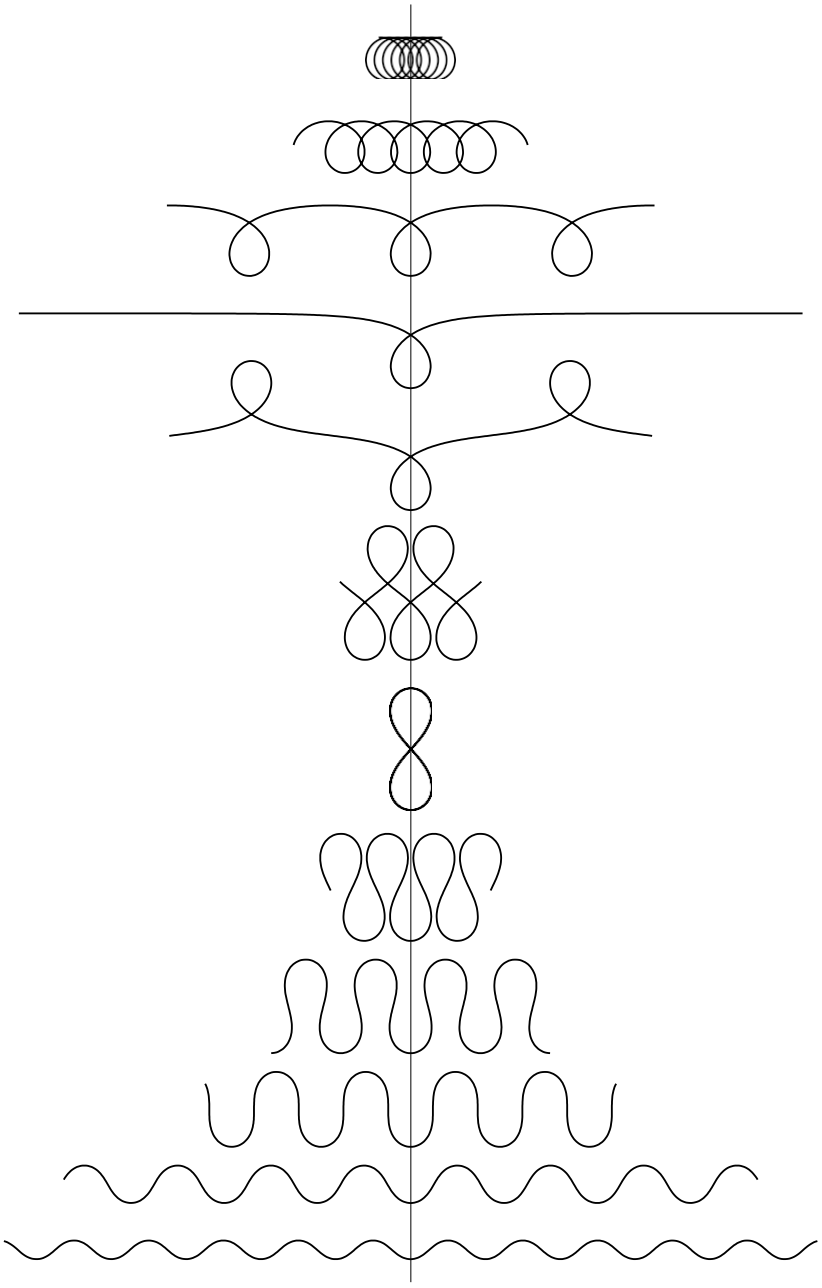

Fig. 33. The evolution of the elastica forms as a function of some parameter λ: λ = 0.1; 0.2; 0.249; 0.25; 0.251; 0.28; 0.3027; 0.35; 0.4; 0.5; 1 and 2 (from top to bottom of the picture) [98, 59].

The elastica forms calculated for different values of the parameter λ: λ = 0.1, λ = 0.2, λ = 0.249, λ = 0.25, λ = 0.251, λ = 0.28, λ = 0.3027, λ = 0.35, λ = 0.4, λ = 0.5, λ = 1 and λ = 2 are shown in Fig. 33. This evolution can qualitatively describe the appearance of the surface craters (λ = 0.249, λ = 0.25) and the atomization of a free liquid surface due to highly-nonlinear wave processes (λ = 0.251, λ = 0.28).

The curves $\lambda = 2;\ 1;\ 0.5;\ 0.4$ and 0.35 qualitatively describe the instability of the interface of two liquids with different densities. The reader can see transforms of the harmonic wave ($\lambda = 2$) into the shock-like wave ($\lambda = 0.5$) and the mushroom-like configurations ($\lambda = 0.4$ and 0.35).

Apparently, the elastica forms can exist in many highly-nonlinear wave systems. Remarkably, the elastica appears as yet another shape of the solution of a fundamental physics problem—the capillary. Pierre Simon Laplace investigated the equation for the shape of the capillary ($\lambda = 0.249$) in his 1807 work [102]. James Clerk Maxwell included the Laplace's result in his article "Capillary Action" in the 9th edition of the Encyclopædia Britannica. Surprisingly, the differential equation for the elastica, expressing curvature as a function of arclength, are equivalent to those of the motion of the pendulum, as worked out by Kirchhoff in 1859 [103].

In spite of the equation for the general elastica being published as early as 1695, the curves had not been accurately plotted until Max Born's 1906 PhD thesis, "Investigations of the stability of the elastic line in the plane and in space" [104]. Years later, Born wrote, "...I felt for the first time the delight of finding a theory in agreement with measurement—one of the most enjoyable experiences I know." [105, p. 21]. Born used the best modern mathematical techniques to address the problem of the elastica, and, among other things, was able to generalize it to the three dimensional case of a wire in space, not confined to the plane.

The forms presented in Figs. 32 and 33 correspond to the static compression of very flexible rods. On the other hand, we found [59, 94-97] that the elastica forms can describe qualitatively the periodic appearance of splashes, drops and bubbles on a liquid surface, as a result of highly-nonlinear effects. In particular, the forms which are intended to describe different forms of rods may be used for the analysis of highly-nonlinear capillary waves. We think that the elastica-like waves and their dynamics describe processes which have been observed in many experiments. In particular, these dynamics can qualitatively describe a transformation of waves into vortices. The theory of the elastica -like travelling waves was developed in [73, 74, 94-97]. In particular, this theory describes the birth of the particles of mass and energy during the origin of the Universe [58-60].

9. Conclusion

We have assumed that the scalar fields of a pre-universe, which are determined by the expressions (1), (2) and (3), leap over infinite distances and permeates all of the spacetime. Due to quantum fluctuations these fields can interact and form a composite field which determines initial conditions of the evolution of the Universe. This approach is quite different from using in the current standard model of cosmology.

Thus, we considered in this work some actual problems of cosmology. On the whole, we developed and corrected some results from [58-60]. More simple picture of pre-universe and its dynamics during the origin of the Universe was constructed. In contrast with [58-60] we did not study here the birth of particles of mass and energy during the origin.

Our aim was to demonstrate that solutions of relatively simple version of nonlinear Klein-Gordon equation can describe the strict sequence of stages of the evolution of some pre-universe into the Universe, if strongly nonlinear effects are taken into account. We link the origin of the Universe with strongly nonlinear interaction of scalar fields existing in some pre-universe. Generally speaking, these fields are separable. However, due to quantum fluctuations the fields can occasionally interact. We considered the interaction of the static and dynamic parts of the initial field. Then the scalar field of quantum fluctuations was introduced and the interaction of the fluctuations and the initial field was studied. The Universe might be originated as a result of similar interactions.

In particular, the eruption depends strongly on the amplitude of quantum fluctuations $\tilde{A}$ and the coefficient of nonlinearity λ. We found that the jump amplification of the scalar field was proportional to $\lambda^{-1}\tilde{A}$. For any λ^{-1} this amplification was approximately $10^{20}\tilde{A}$. Thus, the scalar field can be amplified extremely as a result of the enough weak quantum action. Together with this we recalled that the basic laws of quantum mechanics are applicable for our analysis. In particular, it is well known that the energy density and the energy pressure of the scalar field depend on derivatives Φ_i^2, Φ_t^2 and the scalar potential $V(\Phi)$. Thus, these density and pressure can increase infinitely in the points of discontinuity. Due to above circumstances our Universe can emerge having practically infinite energy and mass. As a result the bubble energy separated from the pre-universe.

A scenario is developed, when the Universe begins from a pre-universe and evolves into a state that differs from initial conditions of the theories of the Big Bang and the inflation.

Acknowledgments

We thank Professor Brian Mace (the University of Auckland) for the support of this research. We had useful discussions of our results with him and Professor Garry Tee (the University of Auckland).

References

[1] F. Hoyle, G. Burbidge, J. V. Narlikar, A Different Approach to Cosmology: From a Static Universe Through the Big Bang Towards Reality, Cambridge University Press (2000).

[2] C. Wetterich, Hot big bang or slow freeze? arXiv:1401.5313 [astro-ph.CO].

[3] A. F. Ali, S. Das, Cosmology from quantum potential, Phys. Lett. B **741**, 276 (2015).

[4] A. Friedmann, Uber die krümmung des raumes (On space curvature), Zeitschrift fur Physik **10**, 377 (1922).

[5] A. Friedmann, Über die möglichkeit einer welt mit konstanter negativer krümmung des raumes, Zeitschrift fur Physik **21**, 326 (1924).

[6] G. Lemaître The beginning of the world from the point of view of quantum theory, Nature **127**, 706 (1931).

[7] A.A. Starobinsky, A new type of isotropic cosmological models without singularity. Phys. Lett. B **91**, 99 (1980).

[8] V. F. Mukhanov, G. V. Chibisov, Quantum fluctuation and nonsingular Universe, JETP Lett. **33**, 532 (1981) [Pisma Zh. Eksp. Teor. Fiz. **33**, 549 (1981)].

[9] Y.-F. Cai, D. A. Easson, R. Brandenberger, Towards a nonsingular bouncing cosmology, arXiv:1206.2382v2 [hep-th].

[10] E. P. Tryon, Is the universe a vacuum fluctuation? Nature **246**, 396 (1973).

[11] A. A. Starobinsky, Spectrum of relict gravitational radiation and the early state of the universe, JETP Lett. **30**, 682 (1979) [Pisma Zh. Eksp. Teor. Fiz. **30**, 719 (1979)].

[12] A. H. Guth, The inationary Universe: A possible solution to the horizon and flatness problems, Phys. Rev. D **23**, 347 (1981).

[13] A. D. Linde, A new inationary universe scenario: A possible solution of the horizon, flatness, homogeneity, isotropy and primordial monopole problems, Phys. Lett. B **108**, 389 (1982).

[14] A. J. Albrecht, P. J. Steinhardt, Cosmology for grand unified theories with radiatively induced symmetry breaking, Phys. Rev. Lett. **48**, 1220 (1982).

[15] D. Atkatz, H. Pagels, Origin of the Universe as a quantum tunneling event, Phys. Rev. D **25**, 2065 (1982).

[16] A. Vilenkin, Creation of Universe from Nothing, Phys. Lett. B **117**, 25 (1982).

[17] L. M. Krauss, A Universe from Nothing, Atria Paperback, NY (2012).

[18] A. Vilenkin, The birth of the inflationary universes, Phys. Rev. D **27**, 2848 (1983).

[19] A.D. Linde, Eternally existing self-reproducing chaotic inflationary universe, Phys. Lett. B **175**, 395 (1986).

[20] A. Vilenkin, Many Worlds in One. Hill and Wang, NY (2006).

[21] S. W. Hawking, The development of irregularities in a single bubble inflationary universe, Phys. Lett. B **115**, 295 (1982); S. W. Hawking, I. G. Moss, J. M. Stewart, Bubble collisions in the very early universe, Phys. Rev. D **26**, 2681 (1982).

[22] A. H. Guth, Quantum fluctuations in cosmology and how they lead to a multiverse, arXiv:1312.7340.

[23] A. Linde, A brief history of the multiverse, arXiv:1512.01203 [hep-th].

[24] M. P. Salem, Bubble collisions and measures of the multiverse, JCAP **1201**, 021 (2012).

[25] J. Garriga, A. Vilenkin, Recycling universe, Phys. Rev. D **57**, 2230 (1998).

[26] M. Bojowald, Absence of a singularity in loop quantum cosmology, Phys. Rev. Lett. **86**, 5227 (2001).

[27] P. J. Steinhardt, N. Turok, A cyclic model of the universe, Science **296**, 1436 (2002).

[28] M. Bojowald, What happened before the Big Bang? Nature Physics **3**, 523 (2007).

[29] P. J. Steinhardt, N. Turok, Endless Universe, Doubleday, NY (2007).

[30] A. Ashtekar, A. Corichi, P. Singh, Robustness of key features of loop quantum cosmology, Phys Rev D **77,** 024046 (2008).

[31] R. Penrose, Cycles of Time: An Extraodinary New View of the Universe. Bodley Head, London (2010).

[32] R. Brandenberger, The matter bounce alternative to inflationary cosmology, arXiv:1206.4196v1 [astro-ph.CO].

[33] A. Barrau, L. Linsefors, Our Universe from the cosmological constant, arXiv:1406.3706 [gr-qc].

[34] S. Gielen, N. Turok, Perfect quantum cosmological bounce, Phys. Rev. Lett. **117**, 021301 (2016).

[35] L. Smolin, Did the Universe evolve? Class. Quantum Grav. **9**, 173 (1992).

[36] L. Smolin, The fate of black hole singularities and the parameters of the standard models of particle physics and cosmology, arXiv:gr-qc/9404011v1.

[37] M. Gasperini, G. Veneziano, String theory and pre-big bang cosmology, arXiv:hep-th/0703055v3; G. Veneziano, A simple/short introduction to pre-Big-Bang physics/cosmology, arXiv:hep-th/9802057v2.

[38] L. Gonzalez-Mestres, BICEP2, Planck, spinorial space-time, pre-Big Bang, https://indico.cern.ch/event/277650/contributions/629783/attachments/505847/698394/ICNFP2014talknewter.pdf.

[39] J. Garriga, A. Vilenkin, J. Zhang, Black holes and the multiverse, arXiv:1512.01819v4 [hep-th].

[40] L. Susskind, The world as a hologram, J. Math. Phys. **36**, 6377 (1995).

[41] A. Ijjas, P. J. Steinhardt, A. Loeb, Inflationary paradigm in trouble after Planck2013, Phys. Lett. B **723**, 261 (2013).

[42] A. Ijjas, P. J. Steinhardt, Implications of Planck2015 for inflationary, ekpyrotic and anamorphic bouncing cosmologies, Class. Quantum Grav. **33**, 044001 (2016); N. Afshordi, J. Magueijo, The critical geometry of a thermal big bang, Phys. Rev. D **94**, 101301 (2016); S. M. Carroll, In What Sense Is the Early Universe Fine-Tuned? arXiv:1406.3057v1 [astro-ph.CO].

[43] Planck Collaboration (P. A. R. Ade *et al.*), Planck intermediate results. XIX. An overview of the polarized thermal emission from Galactic dust, A&A **576**, A104 (2015).

[44] J. R. Gott, T.S. Statler, Constraints on the formation of bubble universes, Phys. Lett. B **136**, 157 (1984).

[45] A. Aguirre, M. C. Johnson, Towards observable signatures of other bubble universes II: Exact solutions for thin-wall bubble collisions, Phys. Rev. D **77**, 123536 (2008).

[46] M. C. Johnson, C. L. Wainwright, A. Aguirre, H. V. Peiris, Simulating the Universe(s) III: Observables for the full bubble collision spacetime, arXiv:1508.03641v1 [hep-th].

[47] R. Chary, Spectral variations of the sky: constraints on alternate Universe, The Astrophysical Journal **817**, 33 (2016).

[48] A. Cho, Controversial test finds no sign of a holographic universe, Science **350**, 1303 (2016).

[49] A.D. Linde, Chaotic inflation, Phys. Lett. B **129**, 177 (1983)

[50] A. Linde, Particle Physics and Inflationary Cosmology, CRC Press (1990).

[51] S. Weinberg, Cosmology, Cambrifge University Press (2008).

[52] D.H.Lyth, A.R.Liddle, The Premordial Density Perturbation. Cosmology, Inflation and Origin of Structure, Cambrifge University Press (2009).

[53] R. Easther, M. Parry, Gravity, parametric resonance, and chaotic inflation, Phys. Rev. D **62**, 103503 (2000).

[54] J. M. Maldacena, Non-Gaussian features of primordial fluctuations in single field in-sationary models, JHEP 0305, 013 (2003) [astro-ph/0210603].

[55] A. Stephon, J. Malecki, L. Smolin, Quantum gravity and inflation, Phys. Rev. D **70**, 044025 (2004).

[56] A. Ashtekar, T. Pawlowski, P. Singh, Quantum nature of the Big Bang, Phys. Rev. Lett. **96**, 141301 (2006).

[57] G. Barenboim, W.-I. Park, W. H. Kinney, Eternal Hilltop Inflation, arXiv:1601.08140v4 [astro-ph.CO].

[58] Sh. U. Galiev, T. Sh. Galiyev, Scalar field as a model describing the birth of the Universe, InterNet. Galiev – Galiyev 18–12–2013 (2013); Sh. U. Galiev, T. Sh. Galiyev, Nonlinear scalar field as a model describing the birth of the Universe, Известия Уфимского Научного Центра Российской Академии Наук (Herald of Ufa Scientific Center, Russian Academy of Sciences (RAS)) **2**, 7 (2014); Sh. U. Galiev,

T. Sh. Galiyev, Coherent model of the births of the Universe, the dark matter and the dark energy. https://researchspace.auckland.ac.nz/handle/2292/23783 (2014).

[59] Sh. U. Galiev, Darwin, Geodynamics and Extreme Waves, Springer (2015).

[60] Sh. U. Galiev, T. Sh. Galiyev, Simple model of the origin of the Universe. Известия Уфимского Научного Центра Российской Академии Наук (Herald of Ufa Scientific Center, Russian Academy of Sciences (RAS)) **4**, 27 (2016).

[61] M. Bellini, Pre-big bang collapsing universe from modern Kaluza-Klein theory of gravity, Phys.Lett. B **705**, 283 (2011).

[62] T.I.Belova, A.E. Kudryavtsev, Solitons and their interactions in classical field theory, Physics-Uspekhi **40,** 359 (1997).

[63] I.Yu. Kobzarev, L.B. Okun, M.B. Voloshin, Bubbles in metastable vacuum, Yad. Fiz. **20**, 1229 (1974); S. R. Coleman,The fate of the false vacuum. 1. Semiclassical theory, Phys.Rev. D **15**, 2929 (1977); M. S. Turner, F. Wilczek, Is our vacuum metastable? Nature **298**, 633 (1982); K. Sato, H. Kodama, M. Sasaki, K.-i. Maeda, Multi-production of universes by first-order phase transition of a vacuum, Phys. Lett. B **108**, 103 (1982); C. Riek *et al*., Direct sampling of electric-field vacuum fluctuations. Science **350**, 420 (2015); Wilczek, The materiality of vacuum, https://pa.as.uky.edu/video/frank-wilczek-materiality-vacuum.

[64] M. Gleiser, Pseudostable bubbles, Phys. Rev. D **49**, 2978 (1994).

[65] P. B. Umbanhowar, F. Melo, H.L. Swinney, Localized excitations in a vertically vibrated granular layer, Nature **382**, 793 (1996).

[66] O. Lioubashevski, Y. Hamiel, A. Agnon, Z. Reches, J. Fineberg, Oscillons and propagating solitary waves in a vertically vibrated colloidal suspension, Phys. Rev. Lett. **83**, 3190 (1999).

[67] C. Suplee, Physics in The 20th Century, Harry N. Abrams *(*1999).

[68] Sh.U. Galiev, 1998 Resonant oscillations of gas sphere, *Proc. 13th Australasian Fluid Mechanics Conference (Melbourne, 13-18 December 1998)* (Monash University), 1027–30; Sh.U. Galiev, Is there some new kind of nonlinear surface waves? Rep. 584, School of Engineering, The University of Auckland, December 1998; Sh.U. Galiev, Unfamiliar waves excited due to parametric and resonant effects, *UpoN'99: Proc. 2nd Intern. Conf. on Unsolved Problems of Noise and Fluctuations (Adelaide,July 1999)* (Adelaide: University of Adelaide), 321–6;

[69] Sh.U. Galiev, Topographic effect in a Faraday experiment. J. Phys. A: Math. Gen. **32**, 6963 (1999).

[70] Sh. U. Galiev, Passing through resonance of spherical waves, Phys. Lett. A **260**, 225 (1999).

[71] Sh. U. Galiev, Unfamiliar vertically excited surface water waves, Phys. Lett. A **266**, 41 (2000).

[72] Sh. U. Galiev, Unfamiliar waves excited due to parametric and resonant effects, Proc. Am. Ins. Phys. **511**, 361 (2000).

[73] Sh. U. Galiev, T. Sh. Galiyev, Nonlinear transresonant waves, vortices and patterns: From microresonators to the early Universe, Chaos **11**, 686 (2001).

[74] Sh. U. Galiev, The theory of non-linear transresonant wave phenomena and an examination of Charles Darwin's earthquake reports, Geophys. J. Inter. **154**, 300 (2003).

[75] N. Graham, N. Stamatopoulos, Unnatural oscillons lifetimes in an expanding background, arXiv:hep-th/0604134v2 .

[76] N.N. Graham, An electroweak oscillon, Phys. Rev. Lett. **98**, 101801 (2007).

[77] E.Farhi, N.Graham, A.H. Guth, N. Iqbal, R.R. Rosales, N. Stamatopoulos, Emergence of oscillons in an expanding background, Phys Rev D **77**, 085019 (2008).

[78] M.A. Amin, R. Easther, H. Finkel, R. Flauger, M.P. Hertzberg, Oscillons after inflation, Phys. Rev. Lett. **108**, 241302 (2012).

[79] L. V. Hau, S. E. Harris, Z. Dutton, C. H. Behroozi, Light speed reduction to 17 metres per second, Nature **397**, 594 (1999).

[80] S. Stock, V. Bretin, F. Chevy, J. Dalibard, Shape oscillation of a rotating Bose-Einstein condensate, Europhys. Lett. **65**, 594 (2004).

[81] P. Ball, Tabletop astrophysics, Nature **411**, 628 (2001).

[82] T. Ohlsson, Relativistic Quantum Physics, Cambridge University Press (2011).

[83] C.E. Niederhaus, J.W. Jacobs, Experimental study of the Richtmyer-Meshkov instability of incompressible fluids, J. Fluid Mech. **485,** 243 (2003).

[84] J. Mureika, D. Stojkovic, Detecting vanishing dimensions via primordial gravitational wave astronomy, Phys. Rev. Lett. **106**, 101101 (2011).

[85] D. Stojkovic, Vanishing dimensions: theory and phenomenology, arXiv:1304.6444 (hep-th).

[86] D. Stojkovic, Vanishing dimensions: a review, Mod. Phys. Lett. A **28** (37), 1330034 (2013).

[87] M. Brooks, Silence is olden, New Scientist **2973**, 34 (2014).

[88] A.J. James, B. Vukasinovich, M.K. Smith, A. Glezer, Vibration-induced drop atomization and bursting, J. Fluid Mech. **476**, 1 (2003).

[89] S. S. Gubser, The Little Book of String Theory, Princeton University Press, Princeton (2010).

[90] E. Siegel, The status of the Universe: 2015, https://medium.com/starts-with-a-bang/the-status-of-the-universe-2015-a5df32d595ae#.7enq4ziyd .

[91] Linde A (2014) Теория инфляционной Вселенной, или теория Мультивселенной (Мультиверса) (Theory of the inflationary Universe, or theory of the Multiuniverse (Multiver)). InterNet. http://scisne.net/a1075 .

[92] L. Smolin, The Trouble with Physics: The Rise of String Theory, the Fall of a Science, and What Comes Next. Houghton Mifflin Harcourt (2006).

[93] G. Ellis, J. Silk, Scientific method: Defend the integrity of physics, Nature **516**, 321 (2014).

[94] H.J. Pain, The Physics of Vibrations and Waves, John Wiley & Sons (1999).

[95] Sh. U. Galiev, Transresonant evolution of wave singularities and vortices. Phys Lett A **311**, 192 (2003); Sh. U. Galiev, Strongly-nonlinear wave phenomena in restricted liquids and their mathematical description. In: Perlidze T (ed) New Nonlinear Phenomena Research, Nova Science Publishers, NY (2008).

[96] Sh. U. Galiev, Modelling of Charles Darwin's earthquake reports as catastrophic wave phenomena. researchspace.auckland.ac.nz/handle/2292/4474 .

[97] Sh. U. Galiev, Геофизические Сообщения Чарльза Дарвина как Модели Теории Катастрофических Волн (Charles Darwin's Geophysical Reports as Models of the Theory of Catastrophic Waves). Centre of Modern Education, Moscow (in Russian) (2011).

[98] R. Levien, The elastica: a mathematical theory, http://levien.com/phd/elastica_hist.pdf .

[99] A. E. H. Love. A Treatise on the Mathematical Theory of Elasticity. Dover Publications, fourth edition (1944); C. Truesdell. Der Briefwechsel von Jacob Bernoulli, chapter Mechanics, especially Elasticity, in the Correspondence of Jacob Bernoulli with Leibniz. Birkh¨auser (1987); C. G. Fraser, Mathematical Techque and Physical Conception in Euler's Investigation of the Elastica. Centaurus **34** (3), 211 (2007).

[100] J. Bernoulli, Quadratura curvae, e cujus evolutione describitur inflexae laminae curvatura, In Die Werke von Jakob Bernoulli, pages 223–227. Birkh¨auser, 1692. Med. CLXX; Ref. UB: L Ia 3, p. 211–212.

[101] L. Euler. Methodus inveniendi lineas curvas maximi minimive proprietate gaudentes, sive solutio problematis isoperimetrici lattissimo sensu accepti, chapter Additamentum 1. eulerarchive.org E065, 1744.

[102] P. S. Laplace. OEuvres compl´etes de Laplace, volume 4. Gauthier-Villars, 1880. Volume 4 of Laplace's Complete Works [19, pp. 349–401].

[103] G. R. Kirchoff, On the equilibrium and the movements of an infinitely thin bar. Crelles Journal, 56 (1859).

[104] M. Born, Untersuchungen ¨uber die Stabilit¨at der elastischen Linie in Ebene und Raum, under verschiedenen Grenzbedingungen. PhD thesis, University of G¨ottingen (1906).

[105] M. Born. My Life and Views. Scribner (1968).